nature cell biology

Article

https://doi.org/10.1038/s41556-024-01456-1

VAMP2 chaperones α-synuclein in synaptic vesicle co-condensates

Received: 19 July 2023

Accepted: 5 June 2024

Published online: 1 July 2024

Check for updates

Chuchu Wang[1,2,3,4], Kai Zhang[1,4], Bin Cai[5], Jillian E. Haller[6], Kathryn E. Carnazza[6], Jiaojiao Hu[1,4], Chunyu Zhao[1,4], Zhiqi Tian[5], Xiao Hu[5], Daniel Hall[5], Jiali Qiang[1,4], Shouqiao Hou[1,4], Zhenying Liu[1,4], Jinge Gu[1,4], Yaoyang Zhang[1,7], Kim B. Seroogy[8], Jacqueline Burré[6], Yanshan Fang[1,7], Cong Liu[1,7], Axel T. Brunger[2,3], Dan Li[9,10] ✉ & Jiajie Diao[5] ✉

α-Synuclein (α-Syn) aggregation is closely associated with Parkinson's disease neuropathology. Physiologically, α-Syn promotes synaptic vesicle (SV) clustering and soluble *N*-ethylmaleimide-sensitive factor attachment protein receptor (SNARE) complex assembly. However, the underlying structural and molecular mechanisms are uncertain and it is not known whether this function affects the pathological aggregation of α-Syn. Here we show that the juxtamembrane region of vesicle-associated membrane protein 2 (VAMP2)—a component of the SNARE complex that resides on SVs—directly interacts with the carboxy-terminal region of α-Syn through charged residues to regulate α-Syn's function in clustering SVs and promoting SNARE complex assembly by inducing a multi-component condensed phase of SVs, α-Syn and other components. Moreover, VAMP2 binding protects α-Syn against forming aggregation-prone oligomers and fibrils in these condensates. Our results suggest a molecular mechanism that maintains α-Syn's function and prevents its pathological amyloid aggregation, the failure of which may lead to Parkinson's disease.

α-Synuclein (α-Syn) is an intrinsically disordered protein that is highly expressed in presynaptic neuronal terminals[1]. It consists of 140 amino acids with a conserved amino (N)-terminal lipid-binding motif followed by an aggregation-prone hydrophobic motif and an acidic carboxy (C)-terminal tail[2,3]. In solution, α-Syn has a propensity to aggregate, forming β-sheet-rich amyloid fibrils in a nucleation-dependent manner[4]. The abnormal aggregation of α-Syn is a pathological hallmark of Parkinson's disease, Lewy body dementia, multiple system atrophy and other synucleinopathies and it plays an essential role in disease initiation and progression[5–7]. α-Syn aggregation is nucleated through liquid–liquid phase separation in vitro[8], which may play an important role in neurodegenerative diseases[9–12]. Synaptic vesicles (SVs) are organized into liquid phases constituting presynaptic clusters of SVs near release sites[13]. Thus, it is critical to identify factors that prevent toxic amyloid formation under physiological conditions.

In contrast with intensive studies on the pathological role of misfolded α-Syn in neurological diseases, the normal functions of α-Syn remain largely unclear[14,15]. Combined in vivo and in vitro experiments

[1]Interdisciplinary Research Center on Biology and Chemistry, Shanghai Institute of Organic Chemistry, Chinese Academy of Sciences, Shanghai, China. [2]Department of Molecular and Cellular Physiology, Stanford University, Stanford, CA, USA. [3]Howard Hughes Medical Institute, Stanford University, Stanford, CA, USA. [4]University of Chinese Academy of Sciences, Beijing, China. [5]Department of Cancer Biology, University of Cincinnati College of Medicine, Cincinnati, OH, USA. [6]Helen and Robert Appel Alzheimer's Disease Research Institute, Brain and Mind Research Institute, Weill Cornell Medicine, New York, NY, USA. [7]State Key Laboratory of Chemical Biology, Shanghai Institute of Organic Chemistry, Chinese Academy of Sciences, Shanghai, China. [8]Department of Neurology, University of Cincinnati College of Medicine, Cincinnati, OH, USA. [9]Bio-X Institutes, Key Laboratory for the Genetics of Developmental and Neuropsychiatric Disorders (Ministry of Education), Shanghai Jiao Tong University, Shanghai, China. [10]Zhangjiang Institute for Advanced Study, Shanghai Jiao Tong University, Shanghai, China. ✉e-mail: lidan2017@sjtu.edu.cn; jiajie.diao@uc.edu

revealed that α-Syn promotes soluble *N*-ethylmaleimide-sensitive factor attachment protein receptor (SNARE) complex assembly through interaction with a vesicular SNARE protein: vesicle-associated membrane protein 2 (VAMP2; also called synaptobrevin-2)[16]. Notably, the levels of VAMP2 and monomeric α-Syn simultaneously decrease with increasing duration of dementia, which implies a potential functional link between VAMP2 and monomeric α-Syn[17]. Moreover, the interaction between α-Syn and VAMP2 with a binding affinity in the micromolar range[18] offers a tool for investigating the cellular functions of α-Syn at the molecular level[19]. However, the molecular basis of the α-Syn–VAMP2 interaction and its influence on the functions of α-Syn remain unknown.

α-Syn binds to highly curved membranes containing negatively charged lipids via its N-terminal domain, which is required to promote the clustering of SVs[20,21]. However, at a high protein-to-lipid ratio, the negatively charged phospholipids in SVs can also induce α-Syn to form aggregation-prone oligomers and facilitate its amyloid aggregation[22,23]. Thus, the question arises of how α-Syn is maintained in a highly dynamic liquid-like state[8,9] without forming pathological fibril aggregation. In this article, we show that the molecular interaction between α-Syn and VAMP2 on SVs participates in the formation of co-condensates of SVs and α-Syn. We also discovered that VAMP2 efficiently prevents α-Syn's oligomerization and amyloid aggregation. Our findings highlight the importance of VAMP2 in chaperoning α-Syn on the SV membrane to maintain a non-pathogenic conformation and promote SV clustering and SNARE complex assembly. This chaperoning activity of VAMP2 reported here represents a unique, non-fusogenic function for SNAREs.

Results

α-Syn and SVs form a co-condensate

First, we re-examined the interaction of α-Syn and SVs containing VAMP2. Detergent is required to purify full-length VAMP2. Since detergent may undergo phase separation under some conditions[24], we used the cytoplasmic domain of VAMP2 ($VAMP2^{1–96}$) that has been reported to anchor on SVs[25] in co-condensation experiments. α-Syn and $VAMP2^{1–96}$ form co-condensates with protein-free SV mimics (SVMs) (Fig. 1a and Extended Data Fig. 1a–e). As a control, $VAMP2^{1–96}$ alone did not induce droplet formation of SVMs (Fig. 1a (top)), whereas a few small droplets were observed for SVMs in the presence of α-Syn (Fig. 1a (middle)). The droplets formed by SVMs and α-Syn substantially increased in size in the presence of $VAMP2^{1–96}$ (Fig. 1a (bottom)), but not with the addition of other presynaptic proteins (Extended Data Fig. 1f). The droplets were formed by multi-component phase separation (also referred to as co-condensation) of SVMs, α-Syn and $VAMP2^{1–96}$, as verified by a fluorescence labelling followed by imaging (Extended Data Fig. 1g). Fluorescence recovery after photobleaching (FRAP) experiments revealed that the droplets formed by the three components exhibited high mobility, like a liquid (Fig. 1b)[9]. Moreover, to further confirm the co-condensation results, we purified SVs (Extended Data Fig. 1h–j) with endogenous full-length VAMP2 from mouse brains and found that α-Syn can co-condensate together with purified SVs (Fig. 1c,d). In the boutons of cultured mouse primary neurons, green fluorescent protein (GFP)-tagged α-Syn (α-Syn-GFP) but not GFP alone co-localized with SVs to form puncta (Fig. 1e). The FRAP experiments in live primary neurons (Fig. 1f) of α-Syn and SVs from the same punctum showed a fluorescence intensity recovery similar to previous results[8,13]. The $t_{1/2}$ of α-Syn-GFP is 18.0 s. The slower fluorescence recovery of SVs was caused by their larger size, which reduces the diffusion speed[26]. Our FRAP speed of α-Syn is comparable to what has been reported for α-Syn phase separation in vitro and in cells[8,27], which is two to three orders of magnitude slower than what has been reported for soluble α-Syn in neurons[28]. Our results support that α-Syn and SVs form liquid-like co-condensates when VAMP2 is on the vesicle surface.

The VAMP2 juxtamembrane region interacts with the α-Syn C terminus

To characterize the structural basis of the interaction between α-Syn and VAMP2, we used solution nuclear magnetic resonance (NMR) spectroscopy. Upon the addition of $VAMP2^{1–96}$ to ^{15}N-labelled α-Syn, the $^{15}N–^{1}H$ heteronuclear single quantum coherence (HSQC) spectrum revealed chemical shifts and cross-peak intensity changes primarily for residues 105–140 of the C-terminal domain of α-Syn (Figs. 2a (left) and 2b (top) and Extended Data Fig. 2a (top)). Considering the relatively small chemical shifts, the overall conformation of α-Syn is largely retained. This finding is consistent with previous studies[16] suggesting that α-Syn binds to VAMP2 mainly through its C-terminal region. However, the NMR chemical shift changes indicate that a more extensive region than that suggested by co-immunoprecipitation studies is involved in binding[19]. Conversely, the addition of α-Syn to ^{15}N-labelled $VAMP2^{1–96}$ resulted in an overall decrease in the cross-peak intensities, and the $VAMP2^{1–96}$ juxtamembrane region exhibited more remarkable chemical shift and intensity variations than those of the other residues (Figs. 2a (right) and 2b (bottom) and Extended Data Fig. 2a (bottom)). This finding implies that $VAMP2^{1–96}$ primarily binds to α-Syn via its juxtamembrane region (Fig. 2c). Previous co-immunoprecipitation studies with full-length VAMP2 in the presence of 0.15% Triton X-100 suggested that there is also an interaction between the N-terminal region of VAMP2 and α-Syn[16], which may be too weak to be detectable by solution NMR. The nearby SNARE motif of VAMP2 also weakly interacted with α-Syn (Fig. 2a–c). Notably, the interfaces identified by NMR chemical shifts include several negatively charged residues (for example, 119D, 126E, 130E and 137E) of the C-terminal region of α-Syn, as well as positively charged residues (for example, 83K, 85K, 86R and 87K) of the juxtamembrane region of VAMP2, indicating that the interaction between VAMP2 and α-Syn is mainly electrostatic, which agrees with an independent study similarly describing an interaction of the juxtamembrane domain of VAMP2 with α-Syn[29].

We further characterized the interaction between α-Syn and VAMP2 on the membrane surface. Using chemical cross-linking coupled with mass spectrometry (XL-MS) profiling interacting lysines on two proteins in the presence of liposomes, we confirmed that the critical region of soluble VAMP2 to interact with α-Syn on membranes is the juxtamembrane region (Fig. 2d and Supplementary Tables 1–3), consistent with the solution NMR data. The majority of α-Syn intra-subunit cross-links are located in the N-terminal region (Supplementary Table 2), whereas most of the α-Syn–VAMP2 inter-subunit cross-links are within its C-terminal region (Supplementary Table 1), which suggests that this region is the focal point of the α-Syn–VAMP2 interaction. Meanwhile, the C-terminal region of α-Syn lacks lysine residues (after residue K97), which prevents interaction of the entire α-Syn C-terminal region with VAMP2 from being captured by XL-MS using lysine-linked reagents. However, the C-terminal interaction region of α-Syn is consistent with previous results[16,19]. Therefore, we only used the on-membrane cross-linking data to confirm the newly discovered interaction between α-Syn and the VAMP2 juxtamembrane region.

Disruption of α-Syn–VAMP2 interaction abolishes co-condensation

Next, we examined whether the α-Syn–VAMP2 interaction mediates α-Syn–SV co-condensation. We prepared a C-terminally truncated variant of α-Syn ($\alpha\text{-Syn}^{1–100}$), which is present within human pathological inclusions[30]. The interaction between α-Syn and VAMP2 was abolished without the α-Syn C-terminal domain, but the SVM binding of α-Syn remained unaffected (Extended Data Fig. 2b,c). Moreover, the truncation efficiently eliminated the co-condensation of α-Syn and SVMs (Fig. 3a (middle) and Extended Data Fig. 2d). In addition, puncta with α-Syn and SVs were eliminated in cultured mouse neurons when expressing similar protein levels of $\alpha\text{-Syn}^{1–100}$ instead of wild-type α-Syn (Fig. 3b and Extended Data Fig. 2e), suggesting that the interaction

https://doi.org/10.1038/s41556-024-01456-1

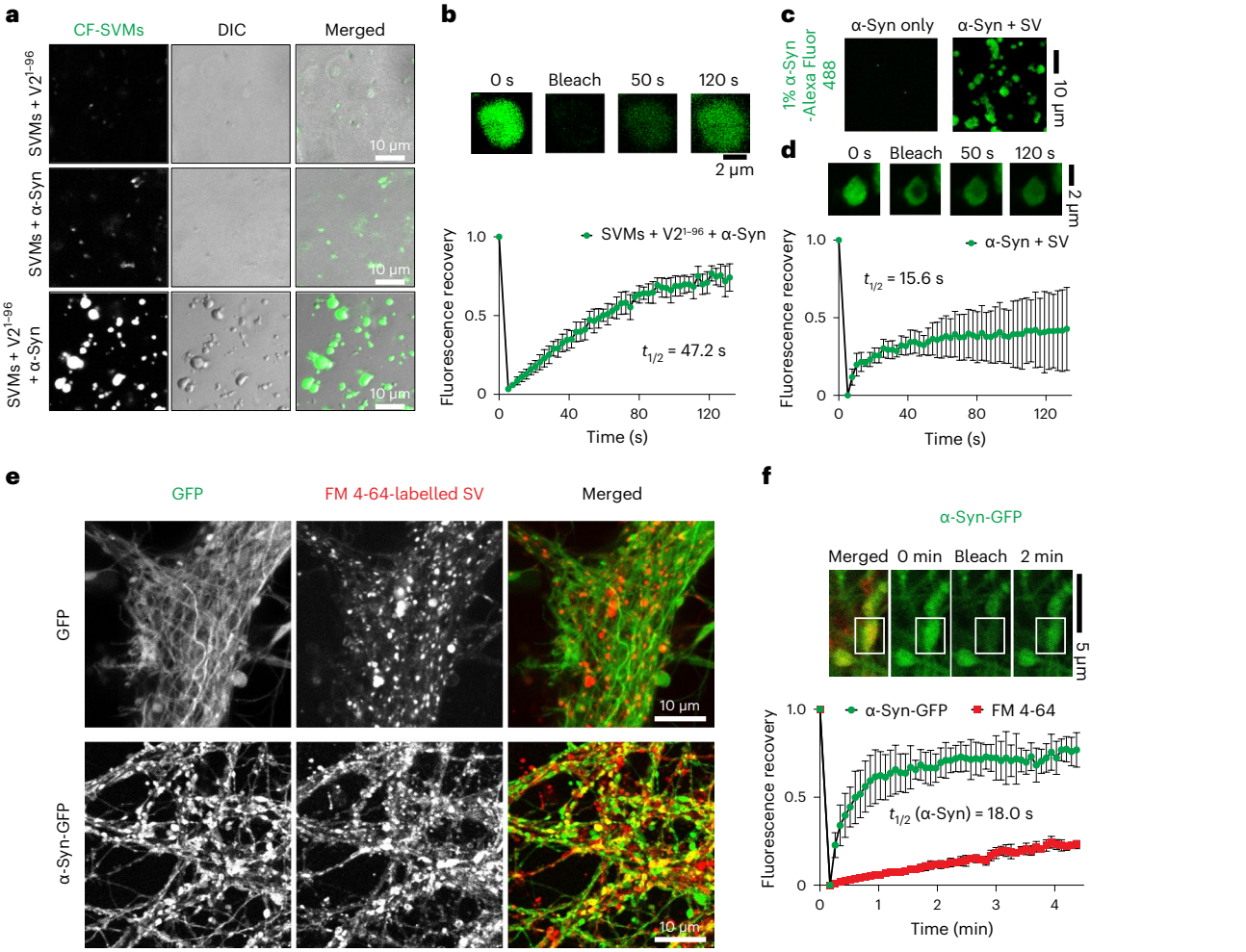

Fig. 1 | SVs and α-Syn co-condense. a, Images of protein-free SVMs (1 mM) in the presence of both VAMP2$^{1–96}$ (V2$^{1–96}$) and α-Syn at a molar ratio of 10:1:1 at room temperature, as well as under SVMs + V2$^{1–96}$ and SVMs + α-Syn conditions. The buffer used was 10 mM HEPES-Na (pH 7.4), 5% (wt/vol) polyethylene glycol 3350 and 5 mM Zn^{2+}. The diameter of the SVMs was ~50 nm (Extended Data Fig. 1a). **b**, FRAP for carboxyfluorescein-labelled SVMs (CF-SVMs) in the presence of both VAMP2$^{1–96}$ and α-Syn. The $t_{1/2}$ was 47.2 s (as determined by fitting a single-term exponential model). Fluorescence images of one droplet at the indicated time points are shown at the top (representative of six FRAP experiments). The data represent means ± s.d. and the error bars (black) represent the s.d. of six independent measurements. **c**,**d**, Images of α-Syn (containing 1% α-Syn-Alexa Fluor 488) with or without isolated SVs from mouse brains (**c**) and FRAP of the α-Syn droplets in the presence of SVs (**d**). The $t_{1/2}$ was 15.6 s. The data represent means ± s.d. and the error bars (black) represent the s.d. of six independent measurements. **e**, Representative images of cortical neurons expressing GFP or α-Syn-GFP loaded with FM 4-64 dye (labelling endocytosed SVs) show puncta of α-Syn and SVs ($n = 6$ independent cultures per condition). **f**, FRAP of α-Syn-GFP and FM 4-64 in a single bouton. Top, representative pseudo-colour images of a string of boutons were selected and a single bouton was selectively photobleached and recovered for the indicated time. Bottom, average FRAP time course of α-Syn-GFP and FM 4-64 in similar sized single boutons to those shown in the top images. The data represent means ± s.d. ($n = 5$ independent measurements on the same bouton for the two fluorescence conditions). DIC, differential interference contrast. Source numerical data are available in Source Data Fig. 1.

between the C-terminal region of α-Syn and VAMP2 is essential for co-condensation of α-Syn and SVs in neurons. We also truncated the juxtamembrane region of VAMP2, which is critical for α-Syn binding. Replacing VAMP2$^{1–96}$ with VAMP2$^{1–78}$ abolished co-condensation of α-Syn and SVMs (Fig. 3a (bottom) and Extended Data Fig. 2d). Moreover, as shown by the solution NMR titration experiments (Extended Data Fig. 2f,g), the acidic residues of E105, D119, E126, E130 and E137 on α-Syn are essential for the interaction with VAMP2. We found that α-Syn^{5A} (E105A, D119A, E126A, E130A and E137A) and α-Syn^{5K} (E105K, D119K, E126K, E130K and E137K) variants disrupt the α-Syn–VAMP2 interaction and abolish co-condensation of α-Syn with SVMs (Fig. 3c) in vitro. α-Syn^{5A} impaired the liquid-like character of co-condensed α-Syn in neurons and α-Syn^{5K} even disrupted it (Fig. 3d,e). The different behaviour of the α-Syn^{5A} variant in vitro versus in the neurons implies that there may be other factors involved in regulating SV co-condensation. Together, our results demonstrate that the interaction between the C-terminal region of α-Syn and the juxtamembrane region of VAMP2 is essential for mediating the co-condensation of α-Syn and SVs.

Disruption of α-Syn–VAMP2 interaction impairs α-Syn function in SV trafficking

We previously showed that α-Syn and VAMP2 cooperate to induce SV clustering[21,31]. Meanwhile, others have shown that α-Syn alone can cluster liposomes[32]. To analyse the influence of VAMP2 on the clustering activity of α-Syn, we conducted a single-vesicle clustering assay using SVMs[33]. We labelled two SVM populations with spectrally distinct fluorescent lipid analogues, DiD and DiI, allowing us to track the location of the free-floating DiD SVMs and to assess the surface coverage of the immobilized DiI SVMs. Interactions between the two populations of SVMs were measured by counting the number of initially free-floating

https://doi.org/10.1038/s41556-024-01456-1

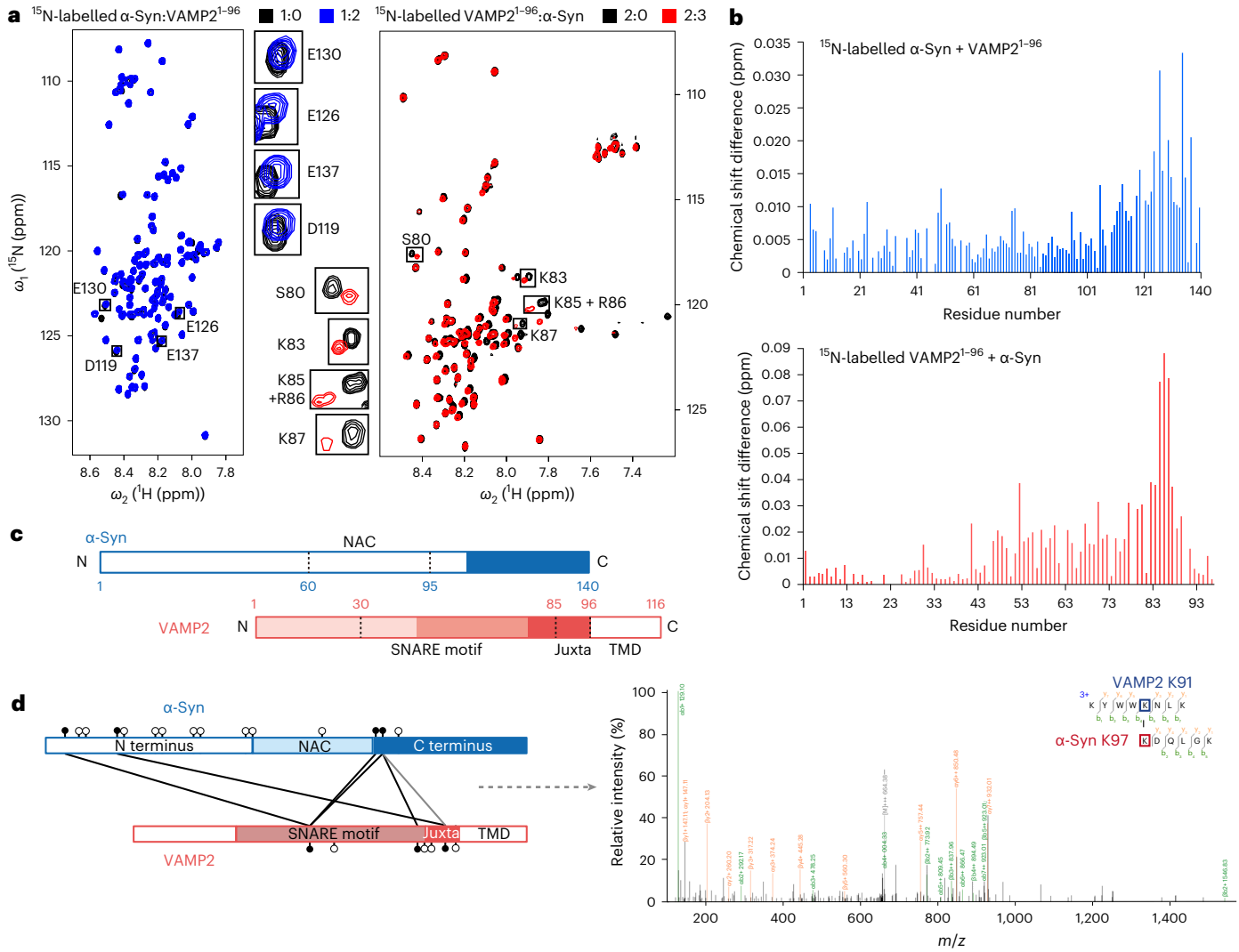

Fig. 2 | The juxtamembrane region of VAMP2 interacts with the C-terminal region of α-Syn. a, Left, overlay of the two-dimensional ^{1}H–^{15}N HSQC spectra of ^{15}N-labelled α-Syn alone (100 μM; black) and in the presence of soluble VAMP2 (blue). Right, overlay of the two-dimensional ^{1}H–^{15}N HSQC spectra of soluble ^{15}N-labelled VAMP2 alone (100 μM; black) and in the presence of α-Syn (red). The residues harbouring large chemical shift changes are magnified. The NMR buffer used was 50 mM NaH_2PO_4 (pH 6.5) with 50 mM NaCl. **b**, Residue-specific changes in the chemical shift of α-Syn signals upon VAMP2 titration (top) and VAMP2 signals upon α-Syn titration (bottom). **c**, Mapping of the interfaces between α-Syn and VAMP2. The C-terminal domain of α-Syn and juxtamembrane region (amino acids 79–96; juxta) of VAMP2 are involved in the interaction between the molecules. The VAMP2 SNARE motif next to the juxtamembrane region also weakly interacts with α-Syn. **d**, Left, diagram of cross-linked lysine pairs of α-Syn and soluble VAMP2, as identified by mass spectrometry. The black and white circles labelled on the protein domain represent cross-linked and unlinked lysine, respectively. Right, a representative second-stage mass spectrometry (MS2) spectrum of cross-linked α-Syn K97 and VAMP2 K91 corresponds to the grey line on the left. The molar ratio of α-Syn (50 μM), $VAMP2^{1–96}$ and PS liposome was 1:1:20 and the cross-linking buffer used was 10 mM HEPES-Na (pH 7.4). NAC, non-amyloid component; TMD, transmembrane domain. Source numerical data are available in Source Data Fig. 2.

DiD SVMs bound to the immobilized DiI SVMs (Extended Data Fig. 3a). Using the clustering assay, we found that α-Syn induced the clustering of protein-free SVMs at a low α-Syn-to-lipid ratio, but this was completely reversed at a high α-Syn-to-lipid ratio (Fig. 4a). In contrast, the reconstitution of a full-length VAMP2 to both DiD and DiI SVMs dramatically boosted α-Syn-mediated SVM clustering in a concentration-dependent manner (Fig. 4b), especially at the high protein-to-lipid ratio. In both cases, a physiological level of negatively charged phospholipids (12% phosphatidylserine (PS)[34]) was required for vesicle clustering (Extended Data Fig. 3b–d). Moreover, vesicle clustering was significantly reduced with $α\text{-Syn}^{1–100}$ or $α\text{-Syn}^{5A}$ variants lacking the residues interacting with VAMP2 (Fig. 4c,d). Thus, the single-vesicle clustering assay revealed that VAMP2 can still maintain the function of α-Syn in clustering SVs even at high α-Syn concentrations usually associated with phase separation[8].

Next, we assessed whether disruption of the interaction between VAMP2 and α-Syn affected its function for SNARE complex assembly. To rule out the possibility that decreased expression levels of $α\text{-Syn}^{1–100}$ or $α\text{-Syn}^{5K}$ variants accounted for this lack of SNARE complex assembly, we transfected HEK293T cells with the three SNAREs syntaxin-1, synaptosomal-associated protein of 25 kDa (SNAP-25) and VAMP2 in addition to increasing amounts of wild-type α-Syn, $α\text{-Syn}^{1–100}$ or $α\text{-Syn}^{5K}$. Even at high levels, compared with wild-type α-Syn, neither $α\text{-Syn}^{1–100}$ (Fig. 4e,f and Extended Data Fig. 4a,b) nor $α\text{-Syn}^{5K}$ (Fig. 4g,h and Extended Data Fig. 4c–f) could support SNARE complex assembly in HEK293T cells or in cultured α-Syn knockout neurons. Furthermore, $α\text{-Syn}^{5K}$ was unable to modulate synaptic transmission as wild-type α-Syn does (Extended Data Fig. 5). These results suggest that the interaction between α-Syn and VAMP2 is essential for maintaining the physiological conformation and function of α-Syn in SV trafficking.

https://doi.org/10.1038/s41556-024-01456-1

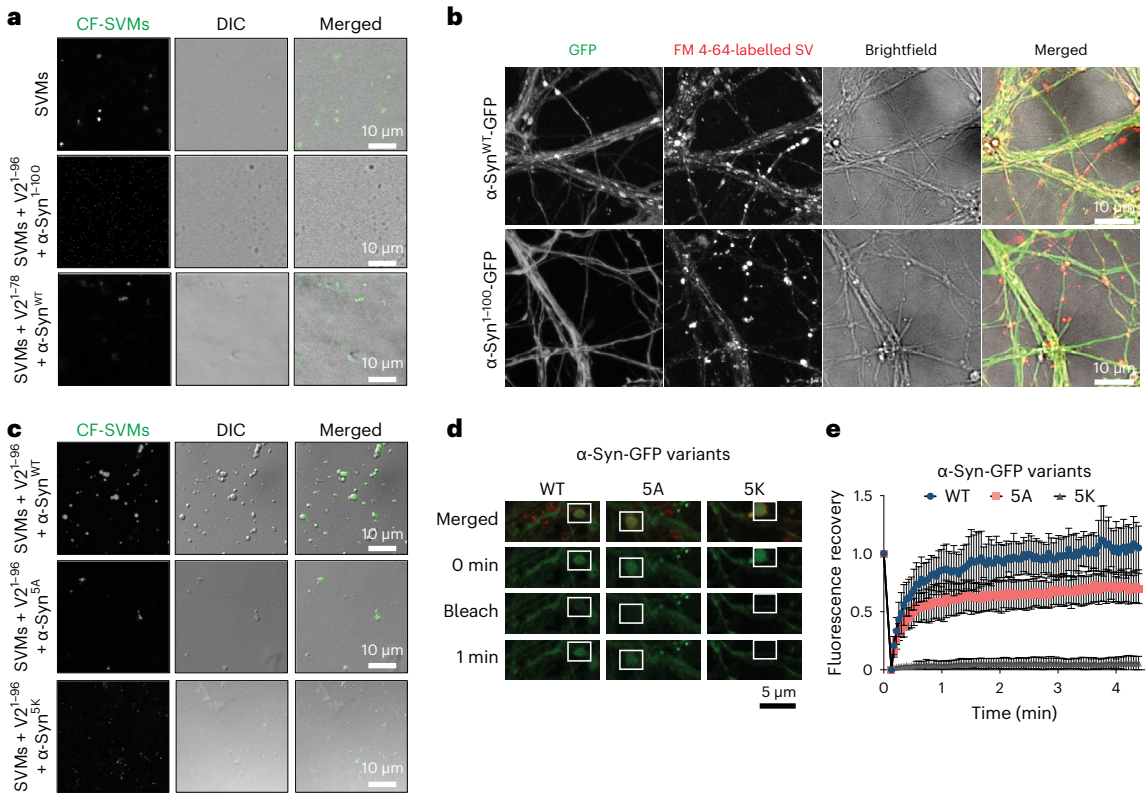

Fig. 3 | Disruption of the α-Syn–VAMP2 interface abolishes co-condensation. **a**, Images of 1 mM CF-SVMs alone and in the presence of VAMP2$^{1–96}$ and α-Syn$^{1–100}$ or VAMP2$^{1–78}$ and wild-type α-Syn. The molar ratio of SVMs:VAMP2:α-Syn was 10:1:1. **b**, Representative images of cortical neurons expressing α-Syn-GFP and α-Syn$^{1–100}$-GFP ($n = 6$ independent cultures per condition) loaded with FM 4-64 dye labelling endocytosed SVs. **c**, Images of 1 mM CF-SVM vesicles alone and in the presence of soluble VAMP2 and α-Syn^{WT}, α-Syn^{5A} (E105A, D119A, E126A, E130A and E137A) or α-Syn^{5K} (E105K, D119K, E126K, E130K and E137K) variants. The molar ratio of SVMs:VAMP2:α-Syn was 10:1:1. **d**, Representative pseudo-colour snapshots of primary neurons expressing different α-Syn-GFP variants in FRAP assay ($n = 8$ random imaging locations). The green colour represents the α-Syn-GFP variants and the red colour represents the FM 4-64 dye. **e**, Results of a representative FRAP experiment on a single bouton (white boxes in **d**) of primary neurons with GFP-linked α-Syn variants. The data represent means ± s.d. and the error bars (black) represent the s.d. of eight independent measurements on the same bouton. Source numerical data are available in Source Data Fig. 3.

VAMP2 prevents α-Syn aggregation and cytotoxicity

Next, we examined how the binding of VAMP2 to α-Syn influences α-Syn amyloid aggregation. Using a thioflavin T (ThT) kinetic assay, which measures α-Syn amyloid fibrils, a kinetics assay and negative-stain electron microscopy, we found that VAMP2$^{1–96}$ reduced α-Syn aggregation in a dose-dependent manner in the presence of PS liposomes, which is critical for α-Syn binding (Fig. 5a,b). In addition to preventing α-Syn fibrillation, the full-length VAMP2 decreased the formation of α-Syn oligomers induced by PS liposomes, as revealed by a cross-linking experiment (Fig. 5c). Expression of VAMP2$^{1–96}$ substantially decreased the formation of insoluble α-Syn aggregation in HEK293T cells (Fig. 5d). A cell viability assay showed that VAMP2 ameliorates the cytotoxicity of α-Syn aggregates to HEK293T cells and cultured primary neurons (Fig. 5e,f). Finally, truncation or mutation affecting the α-Syn-binding region of VAMP2 (VAMP2$^{1–78}$ or VAMP2$^{(1–96)5A}$) decreased the inhibitory effects of VAMP2 on α-Syn aggregation (Fig. 5g,h and Extended Data Fig. 6a,b), which agrees with the FRAP results showing that α-Syn^{5A} with decreased binding to VAMP2 assumes a less liquid state, presumably via aggregation (Fig. 5d,e and Extended Data Fig. 2f,g). α-Syn$^{1–100}$ showed more α-Syn amyloid aggregation in neurons after long-term expression (Extended Data Fig. 6c). Together, these results suggest that VAMP2 chaperones α-Syn on SVM membranes to prevent its oligomerization and amyloid aggregation.

Discussion

Biologically, the juxtamembrane region of VAMP2 for α-Syn interaction may imply a possible regulatory mechanism in SV trafficking and SV clustering at synaptic boutons. The juxtamembrane region of VAMP2 interacts with the SV membrane, which may decrease SNARE complex assembly[25,35]. Therefore, by competing with the interaction between the VAMP2 juxtamembrane region and the SV membrane, α-Syn may promote SNARE complex assembly, thereby regulating synaptic neurotransmitter release. Our earlier findings demonstrated an essential role of VAMP2 in α-Syn-induced SV clustering[21,31], whereas other studies showed that α-Syn alone, synapsin alone or both together can cluster liposomes[13,32]. Here we reconciled these contradictory findings by showing how VAMP2 can maintain the physiological conformation of α-Syn even at high concentrations. Our results agree well with an independent study[29], not only showing that VAMP2 can promote the co-condensation of α-Syn and SVs, but also that the region responsible for SV–α-Syn co-condensate formation is located at the juxtamembrane domain of VAMP2. In addition to SV clustering, α-Syn promotes SNARE complex assembly[36].

For all of the in vitro experiments, we only included α-Syn, VAMP2 and SVM. α-Syn^{5A} effectively disrupts the co-condensation and vesicle clustering in vitro by using either VAMP2$^{1–96}$ (Fig. 3c) or full-length VAMP2 (Fig. 4d). Meanwhile, in synaptic boutons, SVs form tight clusters near presynaptic release sites that are interconnected by highly abundant proteins with multivalent low-affinity interactions[37,38]. However, recent evidence suggests that these synaptic clusters consisting of primed SVs (readily releasable pool) and reserve pools are more dynamic than was previously thought[39], consistent with the notion of a liquid-like co-condensate of SVs and protein components.

https://doi.org/10.1038/s41556-024-01456-1

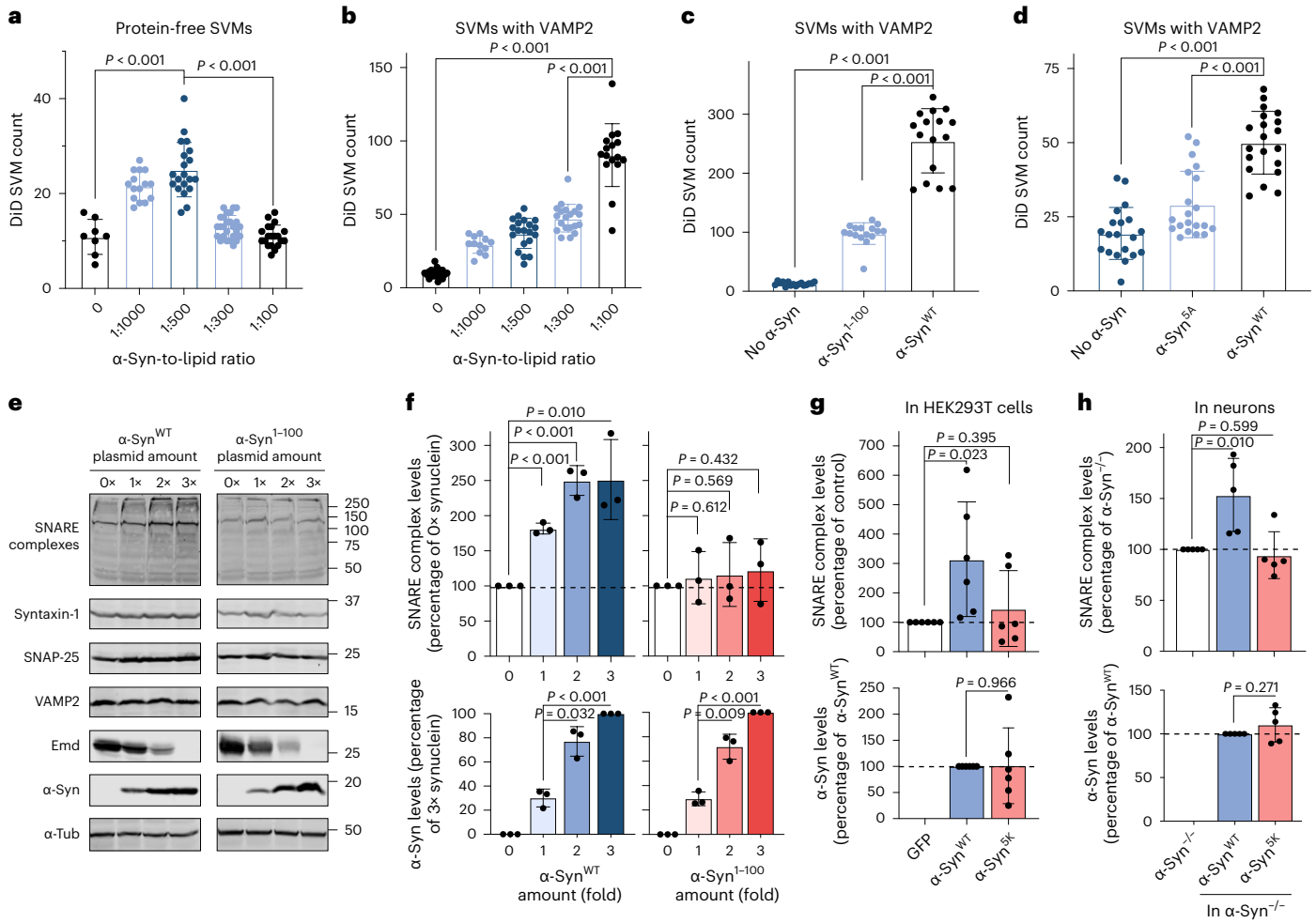

Fig. 4 | Disruption of the α-Syn–VAMP2 interface impairs the α-Syn function of SV trafficking. a, Numbers of interacting DiD-labelled protein-free SVMs on the imaging surface with various protein-to-lipid ratios. **b**, Numbers of interacting DiD-labelled SVMs reconstituted with full-length VAMP2 on the imaging surface with various protein-to-lipid ratios. **c**,**d**, α-Syn$^{1–100}$ (**c**) and α-Syn^{5A} (**d**) reduced the clustering of DiD-labelled SVMs reconstituted with full-length VAMP2. In **a**–**d**, the bar graphs show quantification of the interacting vesicles, where the data represent means ± s.d. and statistical significance was determined by unpaired two-tailed *t*-test (*n* (left to right) = 8, 15, 20, 26 and 20 in **a**, 20, 12, 20, 20 and 16 in **b**, 16 in **c** and 20 in **d** (*n* refers to the number of random imaging locations in the same sample channel)). **e**–**h**, Effects of wild-type α-Syn and α-Syn$^{1–100}$ (**e**,**f**) or α-Syn^{5K} (**g**,**h**) on α-Syn-mediated catalysis of SNARE complex assembly, measured via the SDS resistance of SNARE complexes in transfected HEK293T cells (**e**–**g**) or α-Syn knockout neurons (**h**). HEK293T cells were co-transfected with constant amounts of syntaxin-1, VAMP2 and SNAP-25 and increasing amounts (zero- to threefold) of wild-type α-Syn or α-Syn$^{1–100}$, along with decreasing amounts of pCMV5-emerald (three- to zerofold, to balance the total DNA amount) (**e**,**f**) or fourfold GFP, wild-type α-Syn or α-Syn^{5K} (**g**). α-Syn knockout primary neurons were transduced with lentiviral vectors expressing wild-type α-Syn or α-Syn^{5K} (**h**). The expression levels of individual SNARE proteins are shown in Extended Data Fig. 4a–d. SNARE complexes and α-Syn were quantified and normalized to control levels. α-tubulin (α-Tub), heat shock cognate 71 kDa protein (Extended Data Fig. 4e) or β-tubulin-III (Extended Data Fig. 4f) was used as a loading control. SNARE complexes were measured as high-molecular-mass bands immunoreactive for SNAP-25, which disappeared upon boiling. The data represent means ± s.d. Statistical significance was determined by unpaired two-tailed *t*-test (*n* = 3, 6 and 5 independent cultures for **f**, **g** and **h**, respectively. Source numerical data and uncropped blots are available in Source Data Fig. 4.

Multi-component phase separation or co-condensation of SVs is mediated by synapsin[13], RIM (Rab3 interacting molecules) and RIM-binding proteins[40], Piccolo[41] and α-Syn. Therefore, in the presence of other factors causing SV co-condensation in vivo, α-Syn^{5A} could contribute to SV co-condensation through the remaining charged C-terminal residues (Fig. 3d,e). Considering the relative location of synapsin[42] or α-Syn[43] proximal or distal to the active zone and their potential interaction[44], we propose that α-Syn and synapsin may cooperate for SV co-condensation in neurons[45].

We not only showed that α-Syn interacts with VAMP2 to form droplets with SVs but also discovered an unexpected role for this interaction in preventing α-Syn pathological aggregation. In neurons, α-Syn exists in equilibrium between cytosolic and membrane-bound states. Cytosolic α-Syn is natively unfolded in a monomeric conformation[1,46], whereas membrane-bound α-Syn adopts an α-helical conformation with spontaneous oligomerization on the membrane[20], which could facilitate amyloid fibril aggregation[23]. The SV membrane-bound form of α-Syn, rather than the cytosolic unfolded form, is thought to act as a SNARE complex chaperone in the presynaptic terminal[16] and delays toxicity and pathology[47]. However, the dynamics of α-Syn on the SV membrane surface and its assembly and dissociation regulation remain unclear. Our results suggest that VAMP2 is essential in maintaining the equilibrium between cytosolic and membrane-bound states of α-Syn. Partially folded α-Syn on membranes can bridge SVs[32,48], whereas large oligomers formed by a high protein-to-lipid ratios fall off the membrane and decrease the capability of SV clustering. By interacting with α-Syn, VAMP2 decreases the size of membrane-induced pathological oligomers, thereby preventing cytosolic α-Syn from forming β-sheet-rich amyloid fibrils (Fig. 5i). Since α-Syn aggregates have been implicated in cellular toxicity by disrupting the integrity of biological membranes[49], the interaction

https://doi.org/10.1038/s41556-024-01456-1

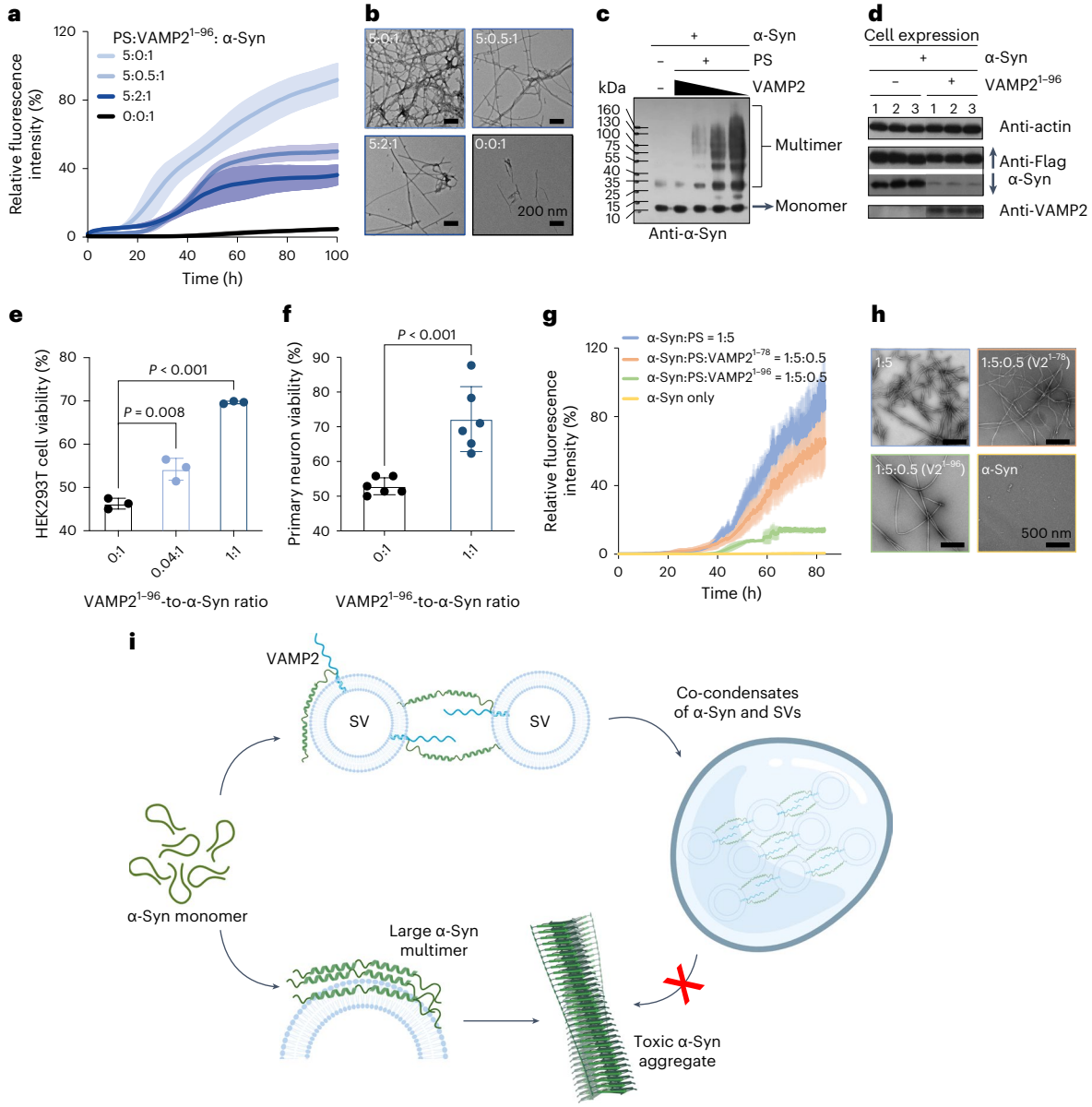

Fig. 5 | VAMP2 prevents α-Syn aggregation and cytotoxicity. a,**b**, ThT spectra (**a**) and electron microscopy images (**b**) showing α-Syn amyloid aggregation in the presence of PS liposomes with or without VAMP2$^{1–96}$. The molar ratios of liposome:VAMP2:α-Syn are indicated. Scale bars, 200 nm. The data represent means ± s.d. and the error bars represent the s.d. of three independent replicates. **c**, Western blot analysis ($n = 3$ independent replicates) of cross-linked α-Syn induced by PS liposomes reconstituted with decreasing concentrations of full-length VAMP2. The falling wedge represents molar ratios of 50 μM α-Syn to full-length VAMP2 (1:2, 1:1, 1:0.5 and 1:0). **d**, Gel image of α-Syn levels in HEK293T cells with or without expression of VAMP2$^{1–96}$. The upward-pointing arrow indicates the supernatant, whereas the downward-pointing arrow designates the pellet containing intact cells. The NP-40 insoluble form of α-Syn was fractionated and quantified by western blot ($n = 2$ independent replicates). **e**,**f**, HEK293T cell (**e**) and primary neuron (**f**) survival measurements with α-Syn and specified VAMP2$^{1–96}$ concentrations. Recombinant α-Syn and VAMP2$^{1–96}$ were added to the cell culture media at the indicated ratios for the cell viability measurements. The data represent means ± s.d. Statistical significance was determined by unpaired two-tailed t-test ($n = 3$ and 6 biologically independent replicates for **e** an **f**, respectively). **g**,**h**, ThT spectra (**g**) and electron microscopy images (**h**) showing α-Syn amyloid aggregation in the presence of PS liposomes with VAMP2$^{1–96}$ or VAMP2$^{1–78}$. The molar ratios of protein and PS lipids are indicated. Scale bars, 500 nm. The data represent means ± s.d. and the error bars represent the s.d. of three independent replicates. **i**, Schematic of how VAMP2 chaperones α-Syn in co-condensates. In neurons, α-Syn exits in dynamic equilibrium between cytosolic and membrane-bound states. Cytosolic α-Syn is intrinsically disordered, whereas membrane-bound α-Syn adopts an α-helical conformation. α-Syn with an α-helical conformation tends to form oligomers on the membrane, which could trigger the formation of β-sheet-rich amyloid fibrils from α-Syn (bottom route). α-Syn can cluster SVs and assist in forming co-condensates and this effect depends on the specific interaction between VAMP2 and α-Syn (top route). Notably, VAMP2 can decrease the size of membrane-induced α-Syn pathological oligomers, thereby preventing cytosolic amyloid aggregation of α-Syn. Schematic created with BioRender.com. Source numerical data and uncropped blots are available in Source Data Fig. 5.

could be a protective presynaptic mechanism. Our findings also show that formation of the co-condensation of α-Syn and SVs depends on a specific protein–protein interaction (between VAMP2 and α-Syn), rather than a non-specific interaction phenomenon, and that this interaction prevents α-Syn pathological aggregation. In cultured neurons, visualization of fluorescently tagged α-Syn in photobleaching experiments showed a similar abundance of α-Syn per SV as VAMP2 (ref. 18), which supports the notion of a preventative effect of α-Syn–VAMP2 interaction. Although it is well known that SNAREs mediate membrane fusion, their possible physiological or pathological function besides

membrane fusion has not been explored. In addition to the above biological implications, this newly discovered non-fusogenic function of VAMP2 in stabilizing α-Syn also holds potential as a platform with which to probe molecular disease mechanisms and identify therapeutic targets for Parkinson's disease.

Online content

Any methods, additional references, Nature Portfolio reporting summaries, source data, extended data, supplementary information, acknowledgements, peer review information; details of author contributions and competing interests; and statements of data and code availability are available at https://doi.org/10.1038/s41556-024-01456-1.

References

1. Burré, J. et al. Properties of native brain α-synuclein. *Nature* **498**, E4–E6 (2013).
2. Maroteaux, L., Campanelli, J. T. & Scheller, R. H. Synuclein—a neuron-specific protein localized to the nucleus and presynaptic nerve-terminal. *J. Neurosci.* **8**, 2804–2815 (1988).
3. Jensen, P. H., Nielsen, M. S., Jakes, R., Dotti, C. G. & Goedert, M. Binding of α-synuclein to brain vesicles is abolished by familial Parkinson's disease mutation. *J. Biol. Chem.* **273**, 26292–26294 (1998).
4. Serpell, L. C., Berriman, J., Jakes, R., Goedert, M. & Crowther, R. A. Fiber diffraction of synthetic α-synuclein filaments shows amyloid-like cross-β conformation. *Proc. Natl Acad. Sci. USA* **97**, 4897–4902 (2000).
5. Goedert, M. Alpha-synuclein and neurodegenerative diseases. *Nat. Rev. Neurosci.* **2**, 492–501 (2001).
6. Jucker, M. & Walker, L. C. Self-propagation of pathogenic protein aggregates in neurodegenerative diseases. *Nature* **501**, 45–51 (2013).
7. Spillantini, M. G. et al. α-Synuclein in Lewy bodies. *Nature* **388**, 839–840 (1997).
8. Ray, S. et al. α-Synuclein aggregation nucleates through liquid–liquid phase separation. *Nat. Chem.* **12**, 705–716 (2020).
9. Mittag, T. & Pappu, R. V. A conceptual framework for understanding phase separation and addressing open questions and challenges. *Mol. Cell* **82**, 2201–2214 (2022).
10. Ray, S. et al. Mass photometric detection and quantification of nanoscale α-synuclein phase separation. *Nat. Chem.* **15**, 1306–1316 (2023).
11. Zbinden, A., Perez-Berlanga, M., De Rossi, P. & Polymenidou, M. Phase separation and neurodegenerative diseases: a disturbance in the force. *Dev. Cell* **55**, 45–68 (2020).
12. Wu, X., Cai, Q., Feng, Z. & Zhang, M. Liquid–liquid phase separation in neuronal development and synaptic signaling. *Dev. Cell* **55**, 18–29 (2020).
13. Milovanovic, D., Wu, Y., Bian, X. & De Camilli, P. A liquid phase of synapsin and lipid vesicles. *Science* **361**, 604–607 (2018).
14. Wang, C. et al. Versatile structures of α-synuclein. *Front. Mol. Neurosci.* **9**, 48 (2016).
15. Burré, J. The synaptic function of α synuclein. *J. Parkinsons Dis.* **5**, 699–713 (2015).
16. Burré, J. et al. α-Synuclein promotes SNARE-complex assembly in vivo and in vitro. *Science* **329**, 1663–1667 (2010).
17. Vallortigara, J. et al. Decreased levels of VAMP2 and monomeric alpha-synuclein correlate with duration of dementia. *J. Alzheimers Dis.* **50**, 101–110 (2016).
18. Fakhree, M. A. et al. The number of α-synuclein proteins per vesicle gives insights into its physiological function. *Sci. Rep.* **6**, 30658 (2016).
19. Sun, J. et al. Functional cooperation of α-synuclein and VAMP2 in synaptic vesicle recycling. *Proc. Natl Acad. Sci. USA* **116**, 11113–11115 (2019).
20. Burré, J., Sharma, M. & Sudhof, T. C. α-Synuclein assembles into higher-order multimers upon membrane binding to promote SNARE complex formation. *Proc. Natl Acad. Sci. USA* **111**, E4274–E4283 (2014).
21. Diao, J. et al. Native α-synuclein induces clustering of synaptic-vesicle mimics via binding to phospholipids and synaptobrevin-2/VAMP2. *eLife* **2**, e00592 (2013).
22. Hu, R. et al. Intrinsic and membrane-facilitated α-synuclein oligomerization revealed by label-free detection through solid-state nanopores. *Sci. Rep.* **6**, 20776 (2016).
23. Galvagnion, C. et al. Lipid vesicles trigger α-synuclein aggregation by stimulating primary nucleation. *Nat. Chem. Biol.* **11**, 229–234 (2015).
24. Arnold, T. & Linke, D. Phase separation in the isolation and purification of membrane proteins. *BioTechniques* **43**, 427–440 (2007).
25. Wang, C. et al. Different regions of synaptic vesicle membrane regulate VAMP2 conformation for the SNARE assembly. *Nat. Commun.* **11**, 1531 (2020).
26. Scott, D. & Roy, S. α-Synuclein inhibits intersynaptic vesicle mobility and maintains recycling-pool homeostasis. *J. Neurosci.* **32**, 10129–10135 (2012).
27. Hardenberg, M. C. et al. Observation of an α-synuclein liquid droplet state and its maturation into Lewy body-like assemblies. *J. Mol. Cell. Biol.* **13**, 282–294 (2021).
28. Spinelli, K. J. et al. Presynaptic alpha-synuclein aggregation in a mouse model of Parkinson's disease. *J. Neurosci.* **34**, 2037–2050 (2014).
29. Agarwal, A. et al. VAMP2 regulates phase separation of alpha-synuclein. *Nat. Cell Biol*. https://doi.org/10.1038/s41556-024-01451-6 (2024).
30. Sorrentino, Z. A. et al. Physiological C-terminal truncation of α-synuclein potentiates the prion-like formation of pathological inclusions. *J. Biol. Chem.* **293**, 18914–18932 (2018).
31. Wang, L. et al. α-Synuclein multimers cluster synaptic vesicles and attenuate recycling. *Curr. Biol.* **24**, 2319–2326 (2014).
32. Fusco, G. et al. Structural basis of synaptic vesicle assembly promoted by α-synuclein. *Nat. Commun.* **7**, 12563 (2016).
33. Diao, J. et al. A single vesicle–vesicle fusion assay for in vitro studies of SNAREs and accessory proteins. *Nat. Protoc.* **7**, 921–934 (2012).
34. Takamori, S. et al. Molecular anatomy of a trafficking organelle. *Cell* **127**, 831–846 (2006).
35. Ellena, J. F. et al. Dynamic structure of lipid-bound synaptobrevin suggests a nucleation-propagation mechanism for *trans*-SNARE complex formation. *Proc. Natl Acad. Sci. USA* **106**, 20306–20311 (2009).
36. Runwal, G. & Edwards, R. H. The membrane interactions of synuclein: physiology and pathology. *Annu. Rev. Pathol.* **16**, 465–485 (2021).
37. Milovanovic, D. & De Camilli, P. Synaptic vesicle clusters at synapses: a distinct liquid phase? *Neuron* **93**, 995–1002 (2017).
38. Chen, X., Wu, X., Wu, H. & Zhang, M. Phase separation at the synapse. *Nat. Neurosci.* **23**, 301–310 (2020).
39. Neher, E. & Brose, N. Dynamically primed synaptic vesicle states: key to understand synaptic short-term plasticity. *Neuron* **100**, 1283–1291 (2018).
40. Wu, X. et al. Vesicle tethering on the surface of phase-separated active zone condensates. *Mol. Cell* **81**, 13–24.e17 (2021).
41. Qiu, H. et al. Short-distance vesicle transport via phase separation. *Cell* **187**, 2175–2193.e21 (2024).
42. Zaltieri, M. et al. α-synuclein and synapsin III cooperatively regulate synaptic function in dopamine neurons. *J. Cell Sci.* **128**, 2231–2243 (2015).

43. Zhang, L. et al. Semi-quantitative analysis of α-synuclein in subcellular pools of rat brain neurons: an immunogold electron microscopic study using a C-terminal specific monoclonal antibody. *Brain Res.* **1244**, 40–52 (2008).
44. Atias, M. et al. Synapsins regulate α-synuclein functions. *Proc. Natl Acad. Sci. USA* **116**, 11116–11118 (2019).
45. Hoffmann, C. et al. Synapsin condensates recruit alpha-synuclein. *J. Mol. Biol.* **433**, 166961 (2021).
46. Theillet, F. X. et al. Structural disorder of monomeric α-synuclein persists in mammalian cells. *Nature* **530**, 45–50 (2016).
47. Burré, J., Sharma, M. & Sudhof, T. C. Definition of a molecular pathway mediating α-synuclein neurotoxicity. *J. Neurosci.* **35**, 5221–5232 (2015).
48. Lautenschlager, J. et al. C-terminal calcium binding of α-synuclein modulates synaptic vesicle interaction. *Nat. Commun.* **9**, 712 (2018).
49. Fusco, G. et al. Structural basis of membrane disruption and cellular toxicity by α-synuclein oligomers. *Science* **358**, 1440–1443 (2017).

Publisher's note Springer Nature remains neutral with regard to jurisdictional claims in published maps and institutional affiliations.

Springer Nature or its licensor (e.g. a society or other partner) holds exclusive rights to this article under a publishing agreement with the author(s) or other rightsholder(s); author self-archiving of the accepted manuscript version of this article is solely governed by the terms of such publishing agreement and applicable law.

© The Author(s), under exclusive licence to Springer Nature Limited 2024

Methods

Lipids

The lipid molecules used in this study were 1,2-dioleoyl-*sn*-glycero-3-phosphocholine (DOPC; 850375), 1,2-dioleoyl-*sn*-glycero-3-phospho-L-serine (DOPS; 840035), 1,2-dimyristoyl-*sn*-glycero-3-phospho-L-serine (DMPS; 840033), 1,2-dioleoyl-*sn*-glycero-3-phosphoethanolamine (DOPE; 850725), 1,2-dioleoyl-*sn*-glycero-3-phosphoethanolamine-*N*-(biotinyl) (Biotinyl PE; 870828), cholesterol (700000) and DOPE-*N*-carboxyfluorescein (810332). All were purchased from Avanti Polar Lipids.

Antibodies

The antibodies used included syntaxin-1 (110011; Synaptic Systems; 1:1,000), SNAP-25 (111011; Synaptic Systems; 1:1,000 and 76422-670; Sternberger Monoclonals; 1:1,000), synaptobrevin-2/VAMP2 (104211; Synaptic Systems; 1:2,000), pCMV5-emerald (Emd) (detected by GFP antibody; JL-8; Clontech; 1:1,000), α-synuclein (610786; BD Transduction; 1:2,000), α-tubulin (12G10; Developmental Studies Hybridoma Bank; 25 ng ml^{-1}), GFP (632381; Clontech; 1:1,000), Hsc70 (P903; made in house; 1:1,000), DYKDDDK (Flag) (2368S; Cell Signaling Technology; 1:1,000), β-Actin (ab8227; Abcam; 1:1,000), synaptophysin (101011; Synaptic Systems; 1:10,000), Rpt4 (sc-65753; Santa Cruz Biotechnology; 1:500), VDAC (4661; Cell Signaling Technology; 1:1,000), SEC61B (14648S; Cell Signaling Technology; 1:1,000), P-S129-α-Syn (51253; Abcam; 1:1,000) and Tuj1 (302302; Synaptic Systems; 1:1,000).

Protein purification

Human wild-type α-Syn, α-Syn$^{1–100}$, α-Syn^{5A} and α-Syn^{5K} were cloned into the pET22 vector. Expression was induced by 1 mM isopropyl -1-thio-D-galactopyranoside (IPTG) at 37 °C for 4 h in *Escherichia coli* BL21-DE3 (CodenPlus). The pellets were lysed in 100 mM Tris-HCl (pH 8.0), 1 mM ethylenediaminetetraacetic acid (EDTA) and 1 mM phenylmethylsulfonyl fluoride (PMSF). The lysates were boiled for 10 min followed by centrifugation at 16,000*g* for 30 min. For wild-type α-Syn and α-Syn^{5A} purification, 20 mg ml^{-1} streptomycin was mixed with the supernatants. After 30 min of centrifugation at 16,000*g*, the pH value of the supernatants was adjusted to 3.5 by 2 M HCl, followed by centrifugation at 16,000*g* for 30 min. Then, the supernatants were dialysed in a buffer containing 25 mM Tris-HCl (pH 8.0) overnight at 4 °C. The dialysed protein solution was further purified by ion-exchange column chromatography (17-5156-01; GE Healthcare), followed by further purification via size exclusion chromatography (Superdex 75; GE Healthcare). For α-Syn$^{1–100}$ and α-Syn^{5K} purification, the supernatants were dialysed against a buffer of 25 mM NaH_2PO_4 (pH 6.0) at 4 °C overnight. The dialysed protein solution was further purified by cation exchange chromatography (HiTrap SP HP; GE Healthcare) and gel filtration via a Superdex 75 column.

The human soluble VAMP2$^{1–96}$, VAMP2$^{1–78}$ and VAMP2^{5A} fused with a His-tag were cloned into the pET31b vector and expressed into inclusion bodies in *E. coli* BL21-DE3. Bacteria were collected by centrifugation after induction by 1 mM IPTG at 37 °C for 6 h at an optical density of 2.0. The pellets were lysed by high pressure in a lysis buffer (50 mM Tris-HCl (pH 7.4), 100 mM NaCl and 1 mM PMSF). The inclusion bodies were centrifuged (16,000*g* for 30 min) and ultrasonically washed twice in 10% Triton X-100 and 1 M NaCl buffer (25 mM Tris-HCl (pH 7.4)) to remove lipid membranes, nucleotides and other proteins. Then, the inclusion bodies were solubilized in 6 M guanidine hydrochloride buffer (25 mM Tris-HCl (pH 7.4)) and purified using HisTrap HP columns (GE Healthcare). The protein was collected in 6 M guanidine hydrochloride buffer (25 mM sodium phosphate (pH 2.0)) and further purified with an RP-HPLC C3 column (Agilent Technology). The lyophilized VAMP2 protein was cleaved by tobacco etch virus protease at 4 °C overnight in buffer (50 mM Tris-HCl (pH 7.4), 100 mM NaCl and 1 mM dithiothreitol (DTT)) to remove the His-tag. VAMP2$^{1–96}$, VAMP2$^{1–78}$ and VAMP2^{5A} were further purified with an RP-HPLC C8 column and lyophilized.

The full-length rat VAMP2 fused with a glutathione *S*-transferase (GST) tag with a thrombin cleavage site was cloned into the pGEX-KGET28a vector. Expression was induced by 0.4 mM IPTG at 25 °C for 12 h in *E. coli* BL21-DE3 (CodenPlus). The pellets were lysed in 50 mM MES (2-(N-morpholino)ethanesulfonic acid) (pH 6.3), 500 mM NaCl, 10% glycerol, 1% Triton X-100, 2 mM DTT and 1 mM PMSF. The lysates were centrifuged at 16,000*g* for 30 min and the pellet was discarded. The supernatant was incubated with 10 ml GST resin (20507ES10; Yeasen Biotechnology) and incubated for 4–6 h at 4 °C. The resin bound with the target protein was washed twice with 40 ml washing buffer (20 mM MES (pH 6.3), 1 M NaCl, 10% glycerol, 0.5% Triton X-100 and 2 mM DTT). Then, the resin was resuspended in 20 ml thrombin cleavage buffer (20 mM Tris-HCl (pH 8.0), 150 mM NaCl, 10% glycerol, 1% β-octyl glucoside and 2 mM DTT) with the addition of 0.5–1.0 U ml^{-1} thrombin (T4648; Sigma-Aldrich) at room temperature for 4 h to remove the GST tag. After running a gel to verify the cleaved protein, the collected flow-through was flash frozen and stored at −80 °C for future use. The full-length VAMP2 construct, Munc18-1, Munc13 and SNAP-25 were kindly gifted by C. Ma (Huazhong University of Science and Technology).

Liposome and SVM preparation

Lipids dissolved in chloroform were evaporated using a dry nitrogen stream. The film of dried lipids was hydrated by adding a ThT or cross-linking buffer solution (indicated below) and then sonicated in a water bath at 65 °C for 10 min. To prepare liposomes of homogenous size, the hydrated lipids were extruded 21 times at 65 °C through a polycarbonate film with a pore size of 50 nm (Whatman Nuclepore Track-Etched Membranes) using an extruder apparatus (610000; Avanti Polar Lipids).

To prepare SVMs, 55 mol% DOPC, 20 mol% DOPS, 15 mol% DOPE and 10 mol% cholesterol were mixed according to a previously published protocol[13]. To prepare the carboxyfluorescein-labelled SVM vesicles (CF-SVMs), 2 mol% DOPE was replaced with 2 mol% DOPE-*N*-carboxyfluorescein in the lipid mixture.

To prepare the DiI and DiD SVMs for single-vesicle clustering experiments, 2 mol% fluorescent dyes (DiI or DiD) and 0.2 mol% Biotinyl PE was added to the SVM lipid mixture. HEPES buffer (25 mM HEPES (pH 7.4) and 90 mM NaCl) was added to the dried tube to hydrate the lipid film. The solution obtained was freeze thawed at least five or six times and stored at −80 °C. Before further experiments, they were filtered through a membrane with a pore size of 50 nm to obtain monodispersed vesicles.

To reconstitute the full-length VAMP2 in vesicles, 65 µl liposomes or SVMs (10 mM lipid in total), 70 µl VAMP2 solution (46.4 µM) and 127.5 µl HEPES buffer were mixed and incubated for 30 min on ice. The mixture was then diluted with the same volume of HEPES buffer. After dialysis in 2 l HEPES buffer overnight, the vesicle solutions were transferred into tubes and stored. The lipid-to-protein ratio was 200:1.

Phase separation assay

CF-SVMs (1 mM) were mixed with wild-type α-Syn, α-Syn$^{1–100}$, α-Syn^{5A} or α-Syn^{5K} variants plus VAMP2$^{1–96}$ or VAMP2$^{1–78}$ or SNAP-25, Munc18 and Munc13 at the indicated molar ratios in buffer A (10 mM HEPES-Na (pH 7.4), 5% (wt/vol) polyethylene glycol 3350 (Sigma-Aldrich) and 5 mM $Zn(Ac)_2$) at room temperature. To characterize the components in SVM droplets, 1% (mol/mol) Alexa Fluor 555-labelled (A20346; Invitrogen) α-Syn-S42C and Alexa Fluor 647-labelled (A20347; Invitrogen) VAMP2-A5C were mixed in buffer A at room temperature. To test whether the purified SVs can form droplets with wild-type α-Syn, SVs were mixed with 100 µM α-Syn (containing 1% α-Syn-Alexa Fluor 488) in buffer A at room temperature. To draw the phase diagram, each sample was prepared in 10 mM HEPES-Na (pH 7.4) and 5 mM $Zn(Ac)_2$. For the turbidity test, 30 µl of each mixture in a 96-well plate was measured using a microplate reader (Thermo Fisher Scientific) at 600 nm and

each measurement contained three replicates. For the imaging experiment, 5 µl of each sample was loaded into an ultra-thin glass-bottom dish (801001; NEST Biotechnology) and imaged using a Leica TCS SP8 confocal microscopy system with differential interference contrast technology and an excitation wavelength of 488 nm.

FRAP experiments

FRAP experiments were performed using a Leica SP8 microscope with a 100× oil objective, which was coupled with a living cell stage for neuron imaging. For the in vitro FRAP assay, 5 µl 1 mM CF-SVM vesicles and VAMP2$^{1–96}$ mixed with α-Syn variants at a molar ratio of 10:1:1 in phase separation buffer at room temperature were loaded into an ultra-thin glass-bottom dish. Circular regions of ~2 µm diameter within droplets of ~4 µm were bleached for 5 s with full laser power, then post-bleach images were acquired at 2.5 s per frame. For the living neuron FRAP assay, recycled SVs were first labelled with FM 4-64 Dye (T13320; Invitrogen), as previously described[50,51]. Circular regions of ~1 µm diameter were bleached for 5 s with full laser power at 488 and 561 nm, separately, and post-images were acquired at 5 s per frame. Images were analysed using Leica Application Suite X software (version 5.2.2) and ImageJ (version 1.54i). For each time point, the intensity was corrected by the intensity of a neighbouring unbleached region (control; ck) and the fluorescence recovery fraction was calculated with the formula $(I_t/I_0)/({}^{ck}I_t/{}^{ck}I_0)$.

SV isolation

We isolated SVs from ~8- to ~12-week-old C57BL6 mice (mixed gender) (Shanghai Lingchang Biotechnology Co. and The Jackson Laboratory) following a previously published protocol[52]. The procedure was performed at 4 °C or on ice with pre-cooled reagents. Eight brains were homogenized in 60 ml 4 mM Na-HEPES (pH 7.4) and 320 mM sucrose buffer with protease inhibitors using glass homogenizers, five strokes with a size A pestle and three strokes with a size B pestle. The homogenate was centrifuged at 816*g* for 10 min. The pellet (P1) was discarded and the supernatant (S1) was centrifuged at 11,200*g* for 15 min. The supernatant (S2) was pipetted off, leaving a pellet of ~2–3 ml. The light portion of the pellet (P2) was gently resuspended using a 10 ml pipette, discarding the dark centre of the pellet. The resuspended P2 pellet (~40 ml) was centrifuged at 13,552*g* for 20 min. The supernatant (S3) was discarded. The resulting pellet (P3), which contained synaptosomes, was resuspended with 4 ml sucrose buffer (with 10X protease inhibitors), then homogenized in 45 ml H_2O using a glass homogenizer (three strokes with the size B pestle). The P3 homogenate was centrifuged at 40,432*g* for 20 min. The pellet (LP1) was discarded. The supernatant (LS1) was centrifuged with an ultra-centrifuge at 280,000*g* for 45 min. The supernatant (LS2) was discarded. The resulting pellet (LP2) was resuspended in 1.5 ml vesicle buffer (20 mM Na-HEPES (pH 7.4) and 90 mM NaCl) and homogenized using a 2 ml glass homogenizer. The LP2 pellet was diluted with vesicle buffer to 5 ml, then thoroughly mixed with 5 ml OptiPrep (D1556; Sigma-Aldrich). Next, gradient ultracentrifugation was performed: the LP2 mixture (containing 50% OptiPrep) was transferred to one SW 40 Ti centrifuge tube, overlayed with 2.5 ml 40% OptiPrep and centrifuged at 285,000*g* for 6 h. Three layers (Extended Data Fig. 1h) of ~200 µl sample were collected carefully.

Fractions of each step were diluted and normalized to a total protein concentration of 50 µg ml^{-1} for western blotting. The antibodies used in this experiment were β-actin for the cytoplasm, synaptophysin for SVs, Rpt4 for the proteosome, VDAC for mitochondria and Sec61B for the endoplasmic reticulum. The bottom layer (Extended Data Fig. 1h) of the suspension was diluted using 25 ml vesicle buffer then centrifuged at 280,000*g* for 40 min. The resulting pellet (purified SVs) was homogenized in 1.5 ml vesicle buffer and drawn through a 20 G hypodermic needle attached to a 3 ml syringe, then drawn through a 27 G needle and expelled. Negative-stain transmission electron microscopy (TEM) was used for quality control and purity assessment of the isolated SVs.

Primary neuron culture experiments

Primary cortical and hippocampal neurons were dissected from E16–E18 embryos of C57BL/6 mice (Lingchang Company) according to the established protocol[50]. Dissociated neurons with a density of 300,000 cells per well were plated onto a 35 mm dish (81158; ibidi). Primary cortical neurons were cultured in serum-free Neurobasal Medium (21103049; Gibco) supplemented with 2% B-27 (17504044; Gibco), 1% GlutaMax (35050061; Gibco) and 1% penicillin–streptomycin at 37 °C under 5% CO_2. At 7 d in vitro, neurons were infected with lentivirus of pLenti-hSyn-GFP, pLenti-hSyn-αSyn-GFP and pLenti-hSyn-αSyn$^{1–100}$-GFP, separately, for 8 d for imaging and 4 and 12 d for the immunoblotting experiments.

To generate lentivirus for infecting primary neurons, HEK293T (CRL-3216; American Type Culture Collection) cells were co-transfected with pLenti-hSyn-GFP[53] or pLenti-hSyn-αSyn-GFP (pLenti-hSyn-αSyn$^{1–100}$-GFP, pLenti-hSyn-αSyn^{5A}-GFP or pLenti-hSyn-αSyn^{5K}-GFP), psPAX2 and pMD2.G at a ratio of 4:2:1 in Opti-MEM medium using Lipofectamine 2000. The culture supernatant was collected at 48 h after transfection and passed through a 0.45 µm filter. Viral particles were concentrated from culture supernatants by Lenti-X Concentrator (Clontech). Viral pellets used for neuronal infection were resuspended in Neurobasal Medium.

Alternatively, mouse cortical neurons were cultured from newborn mice. Brain regions were dissected in ice-cold Hank's Balanced Salt Solution, dissociated by trypsinization (0.05% trypsin-EDTA for 10 min at 37 °C), tritrated with a siliconized pipette and plated (100 µl) onto a 12 mm coverslip (for immunofluorescence) or on 24-well plastic dishes that had been coated for at least 30 min with Matrigel (BD Biosciences). Plating medium (Minimum Essential Medium (Gibco) supplemented with 5 g l^{-1} glucose, 0.2 g l^{-1} $NaHCO_3$ (Sigma-Aldrich), 0.1 g l^{-1} transferrin (Calbiochem), 0.25 g l^{-1} insulin (Sigma-Aldrich), 0.3 g l^{-1} L-glutamine (Gibco) and 10% foetal bovine serum) was replaced with growth medium (Minimum Essential Medium (Gibco) containing 5 g l^{-1} glucose, 0.2 g l^{-1} $NaHCO_3$ (Sigma-Aldrich), 0.1 g l^{-1} transferrin (Calbiochem), 0.3 g l^{-1} L-glutamine (Gibco), 5% foetal bovine serum, 2% B-27 supplement (Gibco) and 2 µM cytosine arabinoside (Sigma-Aldrich)) 24–48 h after plating. Neuronal cultures were transduced with recombinant lentiviruses and/or used for the experiments as indicated.

For the generation of lentiviral particles, HEK293T cells were transfected with complementary DNA using calcium phosphate produced in house: 1 h before transfection, 25 µM chloroquine in fresh media was added. DNA was incubated for 1 min at room temperature in 100 mM $CaCl_2$ and 1× HBS (25 mM HEPES (pH 7.05), 140 mM NaCl and 0.75 mM Na_2HPO_4) and the transfection mix was then slowly added to the cells. The medium was replaced with fresh medium after 6 h. Cells were collected or used for the experiments as indicated 2 d after transfection. For lentivirus production, HEK293T cells were transfected with equimolar amounts of lentiviral vector FUW containing myc-tagged α-Syn, pMD2-G-VSVg, pMDLg/pRRE and pRSV-Rev. Medium containing the viral particles was collected 48 h later and centrifuged for 10 min at 2,000 rpm to remove cellular debris. Viral particles were subsequently concentrated tenfold by centrifugation.

Solution NMR spectroscopy

^{15}N-labelled α-Syn or VAMP2$^{1–96}$ for NMR analysis were concentrated to 100 µM in a 50 mM sodium phosphate buffer (pH 6.5) containing 50 mM NaCl and 10% D_2O (vol/vol). Unlabelled VAMP2$^{1–96}$ (200 µM), α-Syn (150 µM), α-Syn$^{1–100}$ (600 µM) or α-Syn^{5A} (100 µM) were used in the different titration assays. The Agilent standard pulse sequence was used to collect the two-dimensional ^{1}H–^{15}N HSQC spectra[54], which were acquired at 25 °C on an 800 MHz Agilent spectrometer equipped with a cryogenic probe (Agilent Technologies) using the VNMRJ (rev.3.2A) software. Backbone resonance assignment of soluble VAMP2 and α-Syn was accomplished according to Biological Magnetic Resonance Bank entries 4272 (ref. 55) and 6968 (ref. 56). NMR data were processed using NMRPipe (build 2018)[57] and analysed with SPARKY (version 3.115)[58].

Cross-linking experiment

Disuccinimidyl suberate (DSS; 21658; Thermo Fisher Scientific; space arm = 11.4 Å) was used as the cross-linker. Each cross-linking reaction contained 50 μM α-Syn, 1 mM DOPS liposomes, 2 mM DSS and 50 μM VAMP2$^{1–96}$ or the specified concentrations of full-length VAMP2 (Fig. 4c) in cross-linking buffer (10 mM HEPES-NaOH (pH 7.4)). All cross-linking samples were incubated at 25 °C for 1 h and the reactions were terminated by adding Tris-buffer (pH 7.4) to a final concentration of 100 mM at 25 °C for 10 min. The cross-linked α-Syn samples were loaded in a 4–20% precast protein improved gel (36231ES10; Yeasen Biotechnology) and processed for western blotting using an α-Syn antibody (Fig. 5c).

XL-MS experiment

The cross-linked samples were denatured in 8 M urea and 100 mM Tris-HCl (pH 8.5), followed by incubation with 10 mM iodoacetamide for 15 min for the alkylation reaction in the dark. Then, the samples were diluted in 2 M urea and 100 mM Tris-HCl (pH 8.5) and digested with trypsin (the molar ratio of protein to trypsin was 50:1) at 37 °C for 16 h, followed by desalting with C18 desalting tips. The digested peptides were analysed by online nanoflow liquid chromatography with tandem mass spectrometry (LC–MS/MS) on an EASY-nLC 1200 System (Thermo Fisher Scientific) connected to a Q Exactive HF-X (Thermo Fisher Scientific) through a nanoelectrospray ion source. The peptides were separated on a nano-column (manually packed with C18 resin; 100 μm × 15 cm; 1.9 μm; 120 Å) and further analysed using an Orbitrap Q Exactive HF-X mass spectrometer equipped with Thermo Fisher Scientific's Xcalibur (version 4.1) software. A 60 min gradient was used in the Nano LC at a flow rate of 300 nl min^{-1}: for 0–4 min, from 5% buffer B (80% acetonitrile and 0.1% formic acid) and 95% buffer A (0.1% formic acid in water) to 20% buffer B; for 4–45 min, from 20% buffer B to 37% buffer B; for 45–53 min, from 37% buffer B to 47% buffer B, and then increasing to 100% buffer B in the next 4 min and staying at 100% buffer B for 3 min. The precursor ion (MS1) was acquired with a scan range of 350–1,500 *m/z* and a resolution of 60,000 and the automatic gain control target was set at 3×10^6. Each full scan was followed by 20 higher-energy collisional dissociation scans at $R = 30{,}000$ and a normalized collision energy of 27. The scan range of product ion (MS2) was 200–2,000 *m/z*, the automatic gain control target was set at 1×10^5 and the maximum injection time was 45 ms.

The cross-linked peptide pairs were identified by pLink (version 1.9)[59]. The searching parameters of pLink set in this study included: (1) 20 ppm for a window of precursor mass tolerance; (2) 10 ppm for a window of fragment mass tolerance; (3) Lys for cross-linking sites of the cross-linker DSS; (4) 138.0680796 Da for xlink mass shift; (5) 156.0786442 Da for monolink mass shift; (6) 57.02146 Da for fixed carbamidomethyl-Cys modification mass shift; (7) 15.99491 Da for variable Met modification mass shift; (8) 4–100 amino acids per chain for peptide length; (9) 400–10,000 Da per chain for peptide mass; and (10) two missed cleavage sites per chain for trypsin digestion of protein. The search results were filtered with a false rate of <5% and *E* values of <0.0001. The pLink readout data were filtered with a score of $<10^{-14}$ and peptides were identified more than three times.

Single-vesicle clustering experiments

The pre-formed DiI and DiD SVMs with or without VAMP2 were used for single-vesicle clustering experiments. In brief, DiI SVMs were first immobilized on the imaging surface of PEGylated quartz slides via a biotin/NeutrAvidin interaction. DiI SVM coverage was confirmed by green laser excitation. After a buffer change, α-Syn (wild-type α-Syn, α-Syn$^{1–100}$ or α-Syn^{5A}) and DiD SVMs at the specified protein-to-lipid ratio were injected into the sample channel and incubated for 30 min to be bound to immobilized DiI SVMs. Before imaging under a wide-field total internal reflection fluorescence microscopy, the channels were washed with HEPES buffer three times to remove free SVMs. The smCamera program (version 1.0) was used to acquire and analyse the images. The clustering number was determined by counting the number of fluorescent spots of the acceptor channel. Random locations were imaged and analysed for each sample channel on the slide.

ThT fluorescence assay

50 μM α-Syn was incubated with the indicated ratios of VAMP2$^{1–96}$, VAMP2$^{1–78}$, VAMP2^{5A} or DMPS liposomes in ThT buffer (25 mM Tris-HCl (pH 7.5) and 0.05% (wt/vol) NaN_3) and 50 μM ThT in a Nunc 384 plate under agitation of 600 rpm (double orbital) at 37 °C. The ThT fluorescence signal was measured using a microplate reader (BMG Labtech) with an excitation wavelength of 440 nm and a recording emission wavelength of 480 nm. Each experiment comprised three replicates.

Negative-stain TEM

Each sample (5 μl) was pipetted onto a carbon-coated copper grid. Then, 3% uranyl acetate (1% for endogenous SVs) was used for negative staining after washing the grid twice with 5 μl H_2O. The grid was air-dried after removing extra uranyl acetate. TEM images were obtained with an FEI electron microscope at 120 kV equipped with a LaB_6 gun and an FEI BM-Eagle charge-coupled device camera.

Cell culture experiments

HEK293T cells (CRL-3216; American Type Culture Collection) were cultured in Dulbecco's Modified Eagle Medium for 18 h, followed by co-transfection of a Flag-α-Syn plasmid and VAMP2$^{1–96}$ plasmid (vector backbone pCAGGS) using PolyJet reagent for 6 h. Cells were collected 46 h after transfection and lysed with the lysis buffer (50 mM Tris-HCl (pH 7.4), 150 mM NaCl, 0.1% NP-40, 5 mM NaF and 1 mM EGTA, 1 mM EDTA, 1 mM PMSF and protease inhibitors cocktail) for 30 min at 4 °C. The lysates were centrifuged at 12,000*g* for 30 min. The pellets were dissolved with denaturing buffer (50 mM Tris-HCl (pH 7.5), 150 mM NaCl, 1% sodium dodecyl sulfate (SDS) and 5 mM EDTA) overnight with agitation at 16 °C and then boiled for 30 min. The primary antibodies used were anti-Flag, anti-actin and anti-VAMP2.

Cell viability experiments

We used the CellTiter 96 AQueous Non-Radioactive Cell Proliferation Assay (MTT) kit (G4100; Promega) to evaluate the cytotoxicity of α-Syn in the absence or presence of VAMP2. Before the toxicity test, HEK293T cells were first plated at 8,000 cells per well in a 96-well plate at a total volume of 90 μl. The cells were cultured in Dulbecco's Modified Eagle Medium with 10% foetal bovine serum for 18 h at 37 °C under 5% CO_2. Primary cortical neurons were cultured from E16–E18 embryos of pregnant Sprague–Dawley rats (Lingchang Company). Dissociated cortical neurons were cultured in a 96-well plate at a density of 5×10^4 cells per well. For the preparation of α-Syn and VAMP2 mixture solutions, 50 μM α-Syn and 0.25 μM α-Syn fibril seeds were placed on a shaker (37 °C and 900 rpm) with VAMP2 at the indicated concentrations in phosphate-buffered saline for 16 h. To initiate the cell viability assay, 10 μl pre-sonicated (20% power; 15 times) mixture was added to each well and treated for 24 h in HEK293T cells or 30 d in neurons at 37 °C under 5% CO_2. Then, 15 μl Dye Solution (G4102; Promega) was applied into each well. After incubation for 4 h at 37 °C, 100 μl Solubilization Solution (G4101; Promega) was added. After further incubation at 16 °C for 12 h, the absorbance reading was collected at 570 nm with a background reading at 650 nm. Four replicates were measured in parallel for each sample. The cell survival rate was normalized using the phosphate-buffered saline-treated cells as 100% viability and 0.1% SDS-treated cells as 0% viability.

Circular dichroism spectroscopy

Wild-type α-Syn or α-Syn$^{1–100}$ (10 μM) was incubated in a buffer solution (10 mM HEPES (pH 7.4)) or with 100 μM DOPC or DOPS liposomes, respectively. Circular dichroism signals were measured from 260 to

190 nm three times with a scanning speed of 0.3 s nm^{-1} and a bandwidth of 1 nm by Chirascan (Applied Photophysics) at 25 °C. The path length of the quartz cuvettes used was 0.5 mm.

Quantitation of SNARE complex assembly

For the α-Syn titration experiments, HEK293T cells were co-transfected with pCMV5-syntaxin1A, -VAMP2 and -SNAP-25A (1:1:1) and an increasing amount of a plasmid encoding human α-Syn. Total DNA was kept constant by balancing α-Syn plasmid with pCMV5-emerald, which expresses a similar-sized GFP-derived protein. Two days after transfection, cells were collected by solubilization in 0.1% Triton X-100 and subjected to immunoblotting. To measure total SNARE protein levels, samples were boiled for 20 min. SDS-resistant SNARE complexes were defined as the immunoreactive material above 40 kDa that was absent from boiled samples. Note that as with all other quantitative immunoblotting experiments, infrared-dye-labelled secondary antibodies were used and signals were measured using an infrared imaging system (Odyssey CLx; LI-COR).

Multi-electrode array

Primary α-Syn knockout neurons were cultured on 48-well CytoView MEA plates (Axion Biosystems) at one P0 pup per plate with 2.67 μg $μl^{-1}$ laminin. Cells were transduced at 5 d in vitro with lentiviral vectors expressing α-Syn or α-Syn^{5K} or empty vector as a control. Spontaneous activity was recorded at 16 d in vitro for 15 min using the Maestro Pro MEA system (Axion Biosystems). The extracellular voltage was recorded at each electrode with a sampling rate of 12.5 kHz. Spikes were identified from the raw signals using a detection threshold set independently for each electrode of ±6× the s.d. of the noise (AxIS Navigator software; version 3.6.2; Axion Biosystems). Electrodes with at least five spikes per minute were considered active electrodes. Wells without active electrodes were excluded from the analyses. Bursts were identified as events with a minimum of five spikes on an individual electrode, with a maximum inter-spike interval of 0.1 s. Neuronal firing properties were analysed using the Neural Metric Tool (version 4.1.1; Axion Biosystems). The weighted mean firing rate is based on only electrodes with an activity greater than the minimum spike rate and it equals the number of spikes divided by the duration of the analysis. The burst frequency equals the total number of single-electrode bursts divided by the duration of the experiment and the burst percentage equals the number of spikes in single-electrode bursts divided by the total number of spikes and then multiplied by 100.

SNARE complex assembly in primary neurons

α-Syn knockout mice were generated by outcrossing αβγ-synuclein triple-knockout mice with wild-type mice[16]. Primary α-Syn knockout neurons cultured on 48-well CytoView MEA plates were harvested at 16 d in vitro. Neuronal lysates were sonicated and separated by sodium dodecyl sulfate polyacrylamide gel electrophoresis and immunoblotted for SNARE complexes (SMI81; Sternberger Monoclonals), α-Syn and Tuj1 (class III β-tubulin).

Animal statement

All animal procedures were performed in accordance with the protocols approved by the animal care committee of the Interdisciplinary Research Center on Biology and Chemistry at the Chinese Academy of Sciences (rat protocol number 20230110001 and mouse protocol number 20230110005), the Stanford Administrative Panel on Laboratory Animal Care institutional guidelines (mouse protocol number 29981) and to National Institutes of Health guidelines and approved by the committee on animal care at Weill Cornell Medicine (mouse protocol no. 2014-0016).

Statistics and reproducibility

Experimental data were analysed and processed in Excel (2021) and plotted using GraphPad Prism (version 10.2.3) using unpaired two-tailed *t*-tests. The number of experiments, sample size and statistical tests are reported in the respective figure captions. All of the in vitro phase separation imaging assays (Figs. 1a,c and 3a,c and Extended Data Fig. 1e–g,j) were performed in at least three independent experimental sessions. The electron microscopy imaging assays (Fig. 4b,h and Extended Data Fig. 6b) were performed in three independent experimental sessions. No statistical method was used to predetermine the sample size, but our sample sizes are similar to those reported in previous publications[16,21]. The data distribution was assumed to be normal, but it was not formally tested. Experiment randomization was not necessary, but in all experiments, control and experimental samples were analysed in parallel. Data collection and analysis were not performed blind to the conditions of the experiments. No data were excluded from the analyses.

Reporting summary

Further information on research design is available in the Nature Portfolio Reporting Summary linked to this article.

Data availability

All of the data are available within the paper or its supplementary materials. The XL-MS raw data and pLink searched data have been uploaded to iProX with the accession number IPX0006924001. Any data supporting the findings of this manuscript are available from the corresponding author upon reasonable request. Source data are provided with this paper.

References

50. Beaudoin, G. M. 3rd et al. Culturing pyramidal neurons from the early postnatal mouse hippocampus and cortex. *Nat. Protoc.* **7**, 1741–1754 (2012).
51. Gaffield, M. A. & Betz, W. J. Imaging synaptic vesicle exocytosis and endocytosis with FM dyes. *Nat. Protoc.* **1**, 2916–2921 (2006).
52. Ahmed, S., Holt, M., Riedel, D. & Jahn, R. Small-scale isolation of synaptic vesicles from mammalian brain. *Nat. Protoc.* **8**, 998–1009 (2013).
53. Chen, Y. et al. Cell-type-specific labeling of synapses in vivo through synaptic tagging with recombination. *Neuron* **81**, 280–293 (2014).
54. Kay, L. E., Keifer, P. & Saarinen, T. Pure absorption gradient enhanced heteronuclear single quantum correlation spectroscopy with improved sensitivity. *J. Am. Chem. Soc.* **114**, 10663–10665 (1992).
55. Hazzard, J., Südhof, T. C. & Rizo, J. NMR analysis of the structure of synaptobrevin and of its interaction with syntaxin. *J. Biomol. NMR* **14**, 203–207 (1999).
56. Bermel, W. et al. Protonless NMR experiments for sequence-specific assignment of backbone nuclei in unfolded proteins. *J. Am. Chem. Soc.* **128**, 3918–3919 (2006).
57. Delaglio, F. et al. NMRPipe: a multidimensional spectral processing system based on UNIX pipes. *J. Biomol. NMR* **6**, 277–293 (1995).
58. Goddard, T. D., & D. G. Kneller. SPARKY 3 (Univ. California, San Francisco, 2008).
59. Fan, S. B. et al. Using pLink to analyze cross-linked peptides. *Curr. Protoc. Bioinformatics* **49**, 8.21.1–8.21.19 (2015).

Acknowledgements

C.L. and D.L. thank the Major State Basic Research Development Program (2019YFE0120600 to C.L.), National Natural Science Foundation of China (82188101 and 32171236 to C.L. and 92353302 and 32170683 to D.L.), Science and Technology Commission of Shanghai Municipality (grant number 22JC1410400 to C.L.), Shanghai Pilot Program for Basic Research—Chinese Academy of Sciences Shanghai Branch (grant number JCYJ-SHFY-2022-005 to C.L.), Shanghai Basic Research Pioneer Project and Chinese Academy of Sciences Project for Young Scientists in Basic Research (grant

number YSBR-095 to C.L.) for support. This work was supported by the National Institutes of Health (R01NS102181, R01NS113960, 1RF1NS126342 and R21NS127939 to J.B. and R01NS121077 to J.D. and J.B.), Selma Schottenstein Harris Lab for Research in Parkinson's and Michael J. Fox Foundation (16661 to J.D. and K.B.S. and 16164 to J.B.). We thank L. Xu for help with the cell culture experiments and Life Science Editors for editing services. Grammarly was used to check the grammar and style of the manuscript.

Author contributions

C.L., A.T.B., D.L. and J.D. designed and directed the study. C.W., J.H., C.Z., Z.T., D.H., J.Q., S.H., Z.L., J.G. and Y.Z. prepared the proteins, performed the cellular and cross-linking experiments and carried out the ThT, circular dichroism, electron microscopy, NMR and mass spectrometry measurements. C.W., K.Z. and Y.F. conducted the cultured neuron experiments. B.C., Z.T. and X.H. performed the single-vesicle experiments. J.E.H., K.E.C. and J.B. analysed SNARE complex assembly and synaptic transmission. C.W., K.B.S., J.B., C.L., A.T.B., D.L. and J.D. analysed the data, discussed the results and wrote the manuscript.

Competing interests

The authors declare no competing interests.

Additional information

Extended data is available for this paper at https://doi.org/10.1038/s41556-024-01456-1.

Supplementary information The online version contains supplementary material available at https://doi.org/10.1038/s41556-024-01456-1.

Correspondence and requests for materials should be addressed to Dan Li or Jiajie Diao.

Peer review information *Nature Cell Biology* thanks the anonymous reviewers for their contribution to the peer review of this work.

Reprints and permissions information is available at www.nature.com/reprints.

https://doi.org/10.1038/s41556-024-01456-1

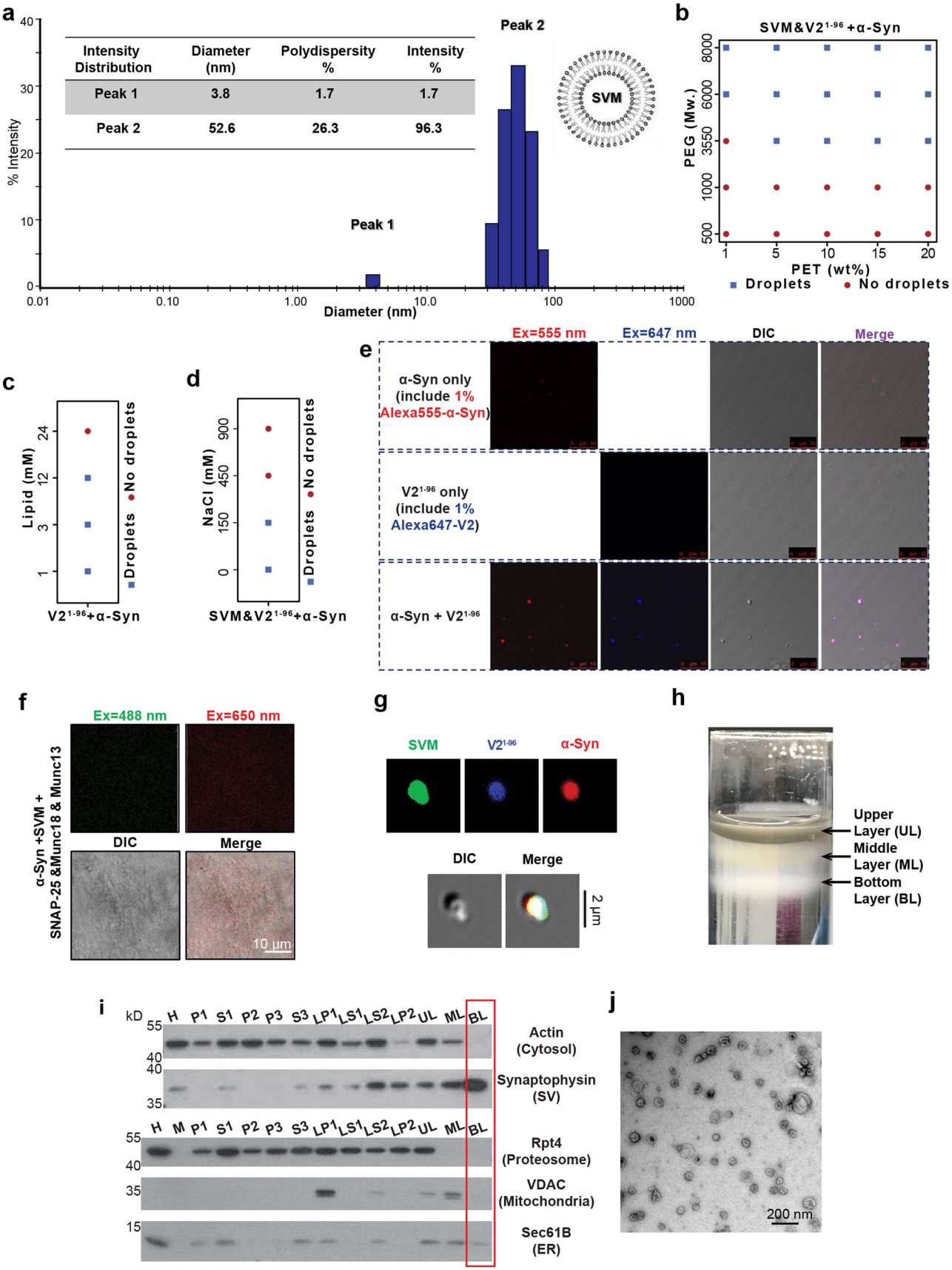

Extended Data Fig. 1 | See next page for caption.

https://doi.org/10.1038/s41556-024-01456-1

Extended Data Fig. 1 | α-Syn, VAMP2, and SVs form a multi-component condensed phase. (**a**) Dynamic light scattering measurement of the size distribution of SVM in solution. **(b)** Molecular weight and concentration of PEG pairs, (**c**) SVM lipid, and (**d**) NaCl concentrations scoring positive (blue dots) or negative (red dots) for the appearance of droplets. 100 μM VAMP21-96, and 100 μM α-Syn were used for all the titrations. Additionally, 1 mM SVMs, 5% (w/v) PEG 3350, or 1 mM SVMs and 5% (w/v) PEG 3350 were used for the titration in (**b**), (**c**), or (**d**), respectively. Fluorescence images of (**e**, top) 100 μM α-Syn (containing 1% Alexa555-α-Syn), (**e**, middle) 100 μM $VAMP2^{1\text{-}96}$ (containing 1% Alexa647-V2), (**e**, bottom) 100 μM α-Syn (containing 1% Alexa555-α-Syn) and 100 μM $VAMP2^{1\text{-}96}$ (containing 1% Alexa647-V2), (**f**) 100 μM α-Syn (containing 1% α-Syn-Alexa488) and 1 mM SVM with 100 μM other synaptic proteins (90 μM SNAP-25, 5 μM Munc18, and 5 μM Munc13), or (**g**) 100 μM α-Syn (containing 1% Alexa555-α-Syn) and 1 mM carboxyfluorescein-green-labeled SVM with 100 μM $VAMP2^{1\text{-}96}$ (containing 1% Alexa647-V2) in the buffer A (10 mM HEPES-Na pH 7.4, 5 mM Zn^{2+}, 5% PEG 3350), respectively. DIC: differential interference contrast. (**h**) The final SV product was fractionated into three fractions by gradient centrifugation. The SVs in the bottom layer were used for experiments. (**i**) Western blot of fractions collected from each step of SV purification. The fraction containing SV is highlighted in red boxes. Other fractions are labeled in abbreviations (see details in Methods). The fractions were immunoblotted for tubulin (cytosol marker), synaptophysin (SV marker), Rpt4 (proteasome marker), VDAC (mitochondria marker), and Sec61B (endoplasmic reticulum marker), respectively. (**j**) Representative negative staining TEM image of endogenous SVs (bottom layer) purified from mouse brains. Uncropped blots are available in the Source Data Extended Data Fig. 1.

https://doi.org/10.1038/s41556-024-01456-1

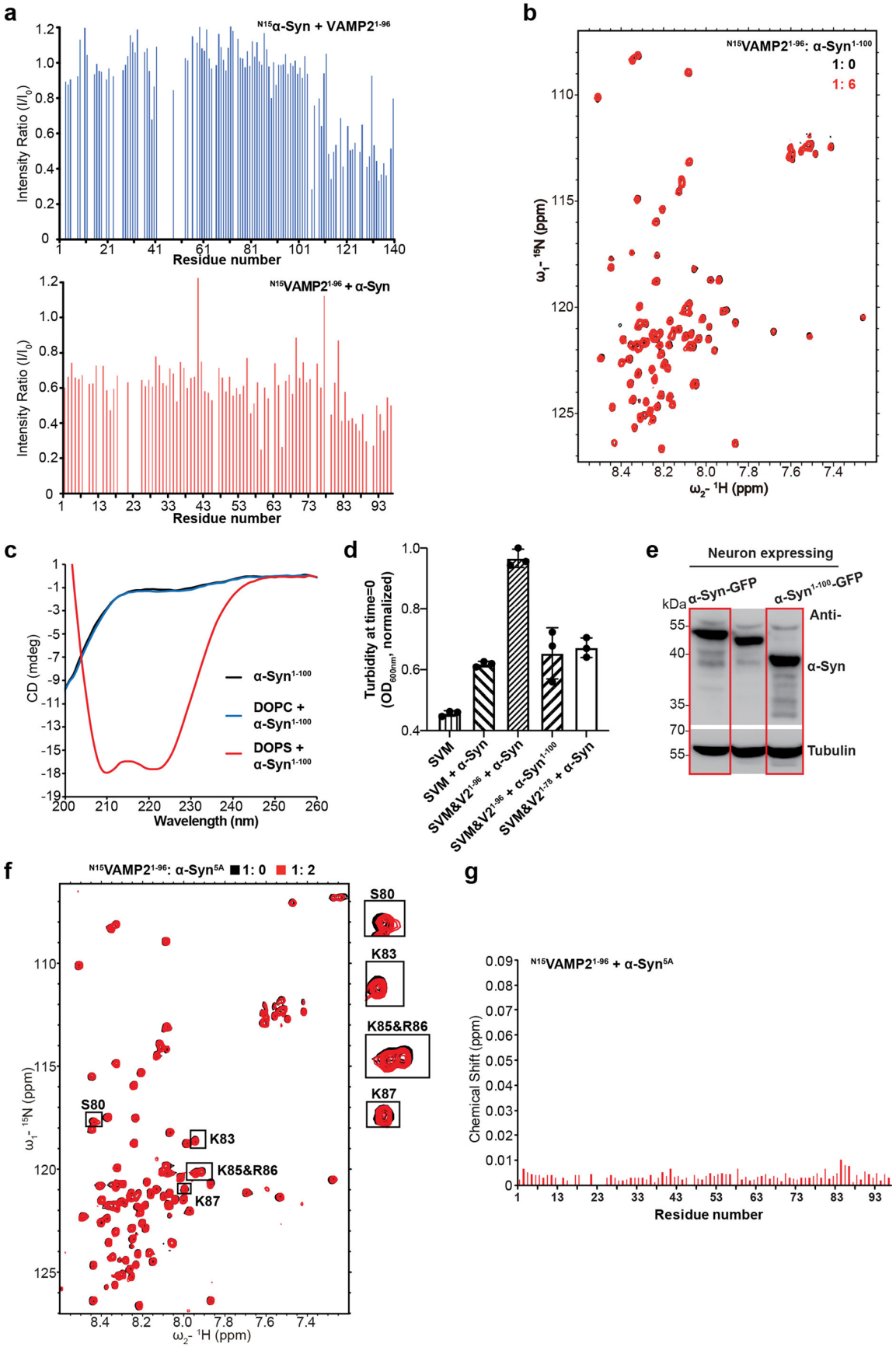

Extended Data Fig. 2 | See next page for caption.

https://doi.org/10.1038/s41556-024-01456-1

Extended Data Fig. 2 | The C-terminal region of α-Syn electrically interacts with the juxtamembrane region of VAMP2. (**a**) Top: residue-resolved relative NMR cross-peak intensity ratios (I/I_0) of 100 μM ^{N15}α-Syn in 200 μM soluble VAMP2 ($VAMP2^{1-96}$) to that in solution. Bottom: residue-resolved relative NMR cross-peak intensity ratios (I/I_0) of 100 μM soluble ^{N15}VAMP2 in 150 μM α-Syn to that in solution. (**b**) The C-terminal region of α-Syn is important for interacting with VAMP2. The 2D ^{1}H-^{15}N HSQC spectrum of ^{15}N-labled soluble VAMP2 (black) and in the presence of $\alpha\text{-Syn}^{1-100}$ alone (red) are almost identical, which validates that the C-terminal end of α-Syn is responsible for the interaction between α-Syn and VAMP2. (**c**) Circular dichroism spectroscopy of $\alpha\text{-Syn}^{1-100}$ alone (black), in the presence of DOPS (red) or DOPC (blue) liposomes, shows that the C-terminal truncation does not influence membrane binding of α-Syn. The molar ratios of VAMP2 to α-Syn are indicated. (**d**) The turbidity was measured for several mixtures: 1 mM SVM alone, SVM mixed with α-Syn only, SVM with $VAMP2^{1-96}$ and α-Syn, SVM with $VAMP2^{1-96}$ and $\alpha\text{-Syn}^{1-100}$, and SVM with $VAMP2^{1-78}$ and α-Syn. The wavelength was 600 nm, and the molar ratio of liposome:VAMP2:α-Syn was 10:1:1. Data are means ± SD; n = 3 replicates. (**e**) Comparison of expression levels of α-Syn-GFP (Fig. 1e) and $\alpha\text{-Syn}^{1-100}$-GFP (Fig. 3b) in cultured cortical neurons by immunoblotting. (**f**) 2D ^{1}H-^{15}N HSQC of ^{15}N-labled soluble VAMP2 only (black) and in the presence of $\alpha\text{-Syn}^{5A}$ (E105A, D119A, E126A, E130A, E137A) alone (red) are nearly identical. (**g**) Per residue chemical shift changes of soluble VAMP2 signals upon $\alpha\text{-Syn}^{5A}$ titration. Source numerical data and uncropped blots are available in the Source Data Extended Data Fig. 2.

https://doi.org/10.1038/s41556-024-01456-1

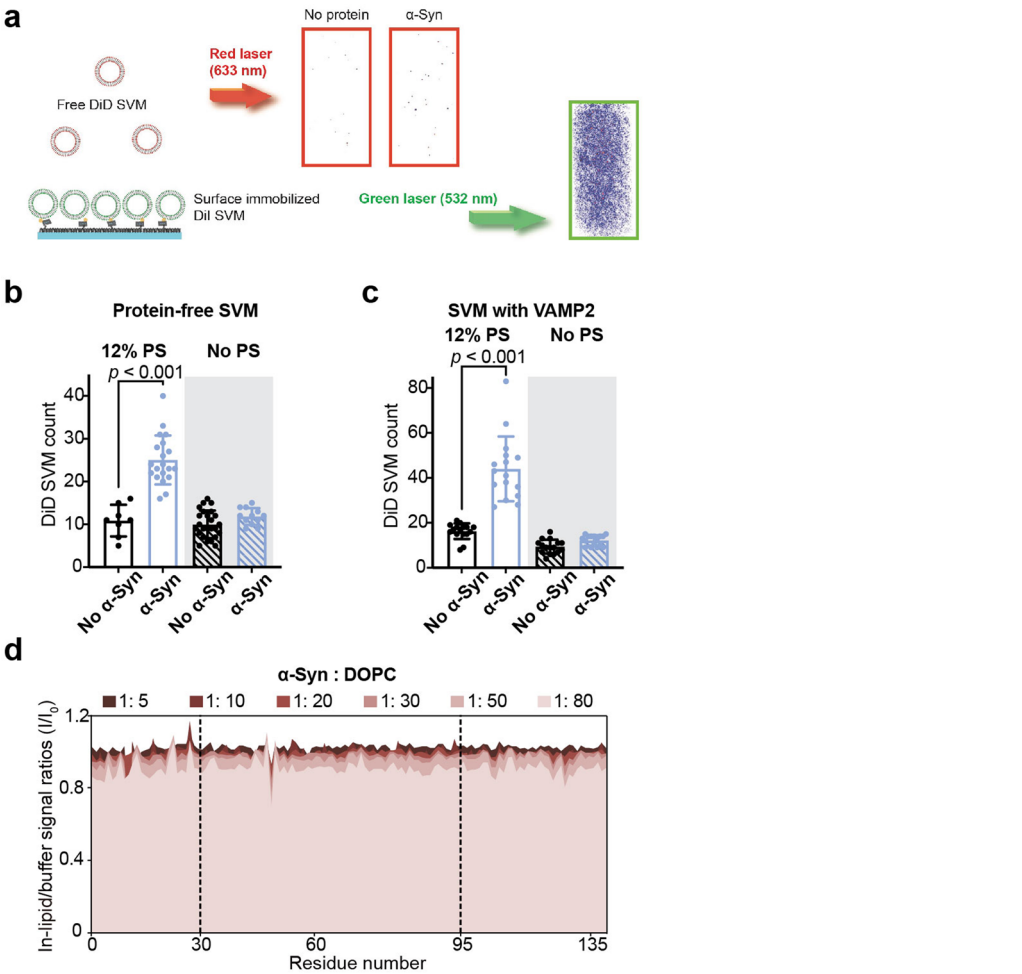

Extended Data Fig. 3 | The negatively charged phosphatidylserine (PS) is important in α-Syn-induced clustering. (**a**) Experimental scheme of single-vesicle assay for monitoring vesicle clustering. A saturated layer of DiI-labeled SVM was immobilized on an imaging surface via biotin–NeutrAvidin interactions. After free-floating DiD-labeled SVM was injected into the sample chamber, clustering in the presence or absence of α-Syn was determined by counting the number of spots arising from the fluorescence emission of DiD upon excitation at 633 nm. (**b**) The numbers of interacting DiD-labeled, protein-free SVMs—with or without PS—interacting on the imaging surface was assessed both in the presence of α-Syn or not. (**c**) The numbers of interacting DiD-labeled, full-length VAMP2 reconstituted SVMs—with or without PS—interacting on the imaging surface was assessed both in the presence of α-Syn or not. (**b**-**c**) Bar graphs: quantification of interacting vesicles; data are means ± SD; unpaired two-tailed *t*-test; n (left to right) = 8, 20, 25, 12, or 16, 16, 16, 16 for (**b**) or (**c**), respectively; n refers to the number of random imaging locations in the same channel. (**d**) Residue-resolved relative NMR signal intensity ratios (I/I_0) of α-Syn titrated by DOPC liposome at indicated protein/lipid molar ratios. Dashed lines highlight the residue positions 30 and 95. Source numerical data is available in the Source Data Extended Data Fig. 3.

https://doi.org/10.1038/s41556-024-01456-1

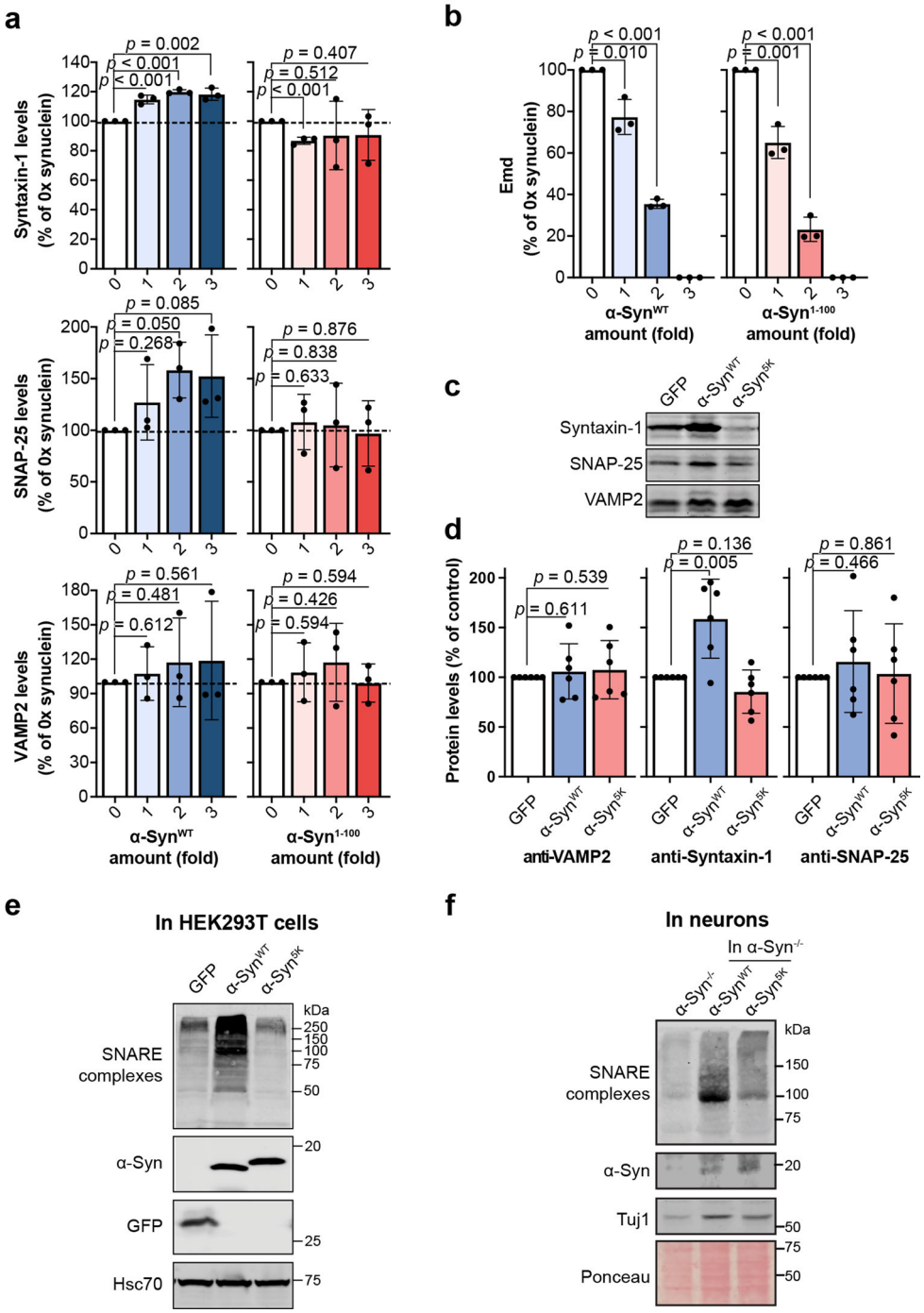

Extended Data Fig. 4 | Disrupting the interface between α-Syn and VAMP2 impairs the catalysis role of α-Syn in SNARE complex assembly. Expression levels of three SNARE proteins in HEK293T cells co-transfected with plasmids expressing (**a**, top; **c**, top; and **d**, middle) syntaxin-1, (**a**, middle; **c**, middle; and **d**, right) SNAP-25, and (**a**, bottom; **c**, bottom; and **d**, left) VAMP2 at a 1:1:1 ratio, together (**a,b**) with an increasing amount (0-3-fold) of α-Syn variant plasmids (WT and α-Syn^{100}), and (**c,d**) with 4-fold expression plasmids of GFP, α-Syn^{WT} and α-Syn^{5K}. Cell lysates were immunoblotted for the indicated SNAREs, followed by quantitation for representative immunoblots (see Fig. 4e). Total expression levels of individual SNARE proteins or balancing pCMV5-emerald in transfected HEK293T cells were analyzed by melting SNARE-complexes in SDS sample buffer (100 °C for 20 min), and quantitated by immunoblotting, normalized to α-tubulin (α-Tub) or heat shock cognate 71 kDa protein. HEK293T cell lysates (**e**) (n = 6 independent replicates) or primary neuron lysates (**f**) (n = 5 independent replicates) were immunoblotted for SNARE complexes and α-Syn followed by quantification and normalization to heat shock cognate 71 kDa protein (Hsc70) or β-tubulin-III (Tuj1) levels. Data shown are means ± SD; unpaired two-tailed *t*-test; n = 3 (**a**,**b**) or 6 (**d**) independent cultures. Source numerical data and uncropped blots are available in the Source Data Extended Data Fig. 4.

https://doi.org/10.1038/s41556-024-01456-1

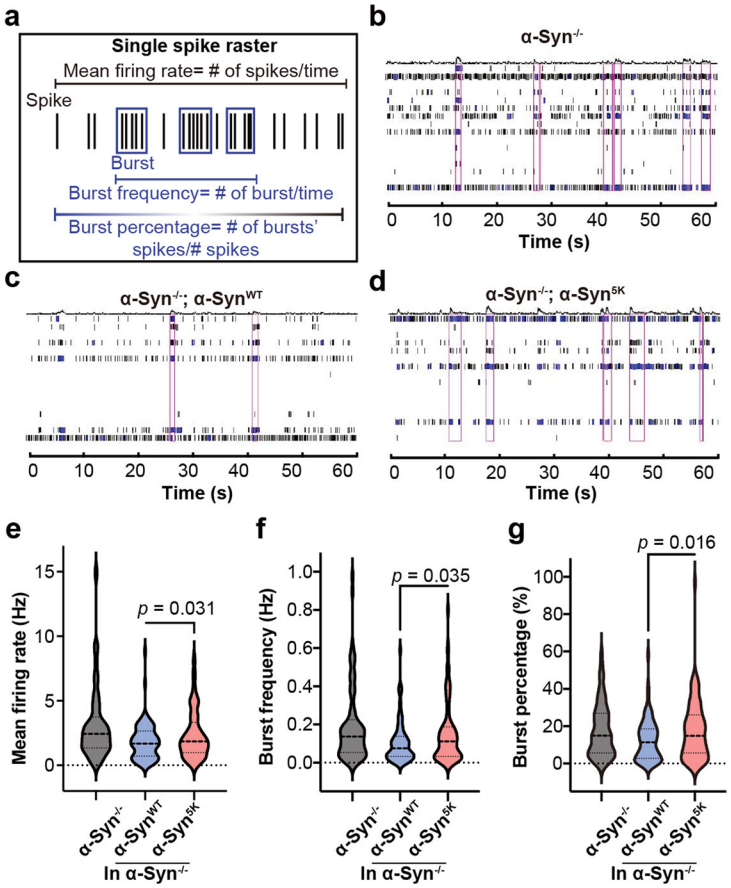

Extended Data Fig. 5 | Disrupting the interface between α-Syn and VAMP2 impairs the role of α-Syn in synaptic transmission. (**a**) Graphic annotation of the multi-electrode array (MEA) assay on cultured primary neurons. (**b-d**) Representative images of conducting MEA assay in the α-Syn knockout neurons (**b**) or knockout neurons expressing wildtype α-Syn (**c**) or α-Syn^{5K} (**d**) mutant. (**e-g**) MEA data from α-Syn knockout neurons or knockout neurons expressing wildtype α-Syn or α-Syn^{5K} mutant were subjected to analysis of mean firing rate (**e**), burst frequency (**f**), and burst percentage (**g**). In the Violin plots, the lower dashed line represents the first quartile, the middle dashed line represents the median, and the upper dashed line represents the third quartile; unpaired two-tailed *t*-test; n (left to right) = 88, 88, 88, or 82, 73, 80 or 84, 80, 86 firing events for (**e**) or (**f**) or (**g**), respectively. Source numerical data is available in the Source Data Extended Data Fig. 5.

https://doi.org/10.1038/s41556-024-01456-1

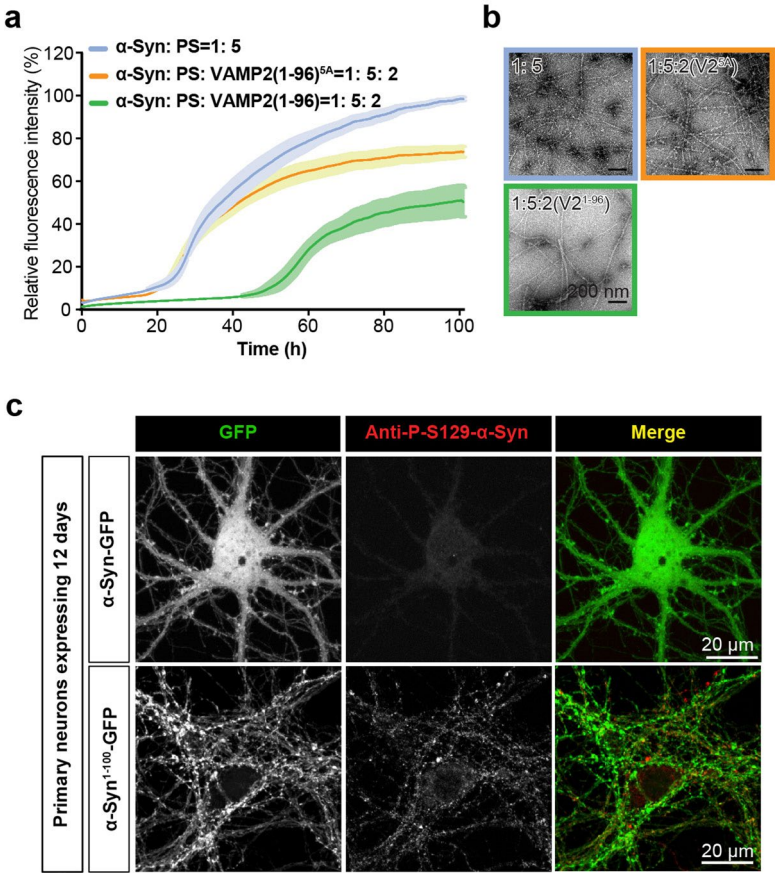

Extended Data Fig. 6 | VAMP2 prevents α-Syn aggregation *in vitro* and in neurons. (**a**) ThT spectra and (**b**) negative staining TEM images show α-Syn (50 μM) amyloid aggregation in the presence of PS liposomes with VAMP2^{5A} (S80A, K83A, K85A, R86A, K87A) mutant or VAMP2. Data are means ± SD; error bars represent the SD of three replicates. (**c**) Immunofluorescence images of hippocampal neurons transfected with the same amount of plasmids of full-length and C-terminally-truncated α-Syn-GFP, respectively, for 12 days with anti-P-S129-α-Syn. This antibody stains the human hippocampus of Parkinson's disease brains but shows no staining in normal brains. Source numerical data is available in the Source Data Extended Data Fig. 6.

nature portfolio

Corresponding author(s): Dan Li, Jiajie Diao

Last updated by author(s): May 29, 2024

Reporting Summary

Nature Portfolio wishes to improve the reproducibility of the work that we publish. This form provides structure for consistency and transparency in reporting. For further information on Nature Portfolio policies, see our Editorial Policies and the Editorial Policy Checklist.

Statistics

For all statistical analyses, confirm that the following items are present in the figure legend, table legend, main text, or Methods section.

n/a	Confirmed
☐	☒ The exact sample size (*n*) for each experimental group/condition, given as a discrete number and unit of measurement
☐	☒ A statement on whether measurements were taken from distinct samples or whether the same sample was measured repeatedly
☐	☒ The statistical test(s) used AND whether they are one- or two-sided *Only common tests should be described solely by name; describe more complex techniques in the Methods section.*
☒	☐ A description of all covariates tested
☒	☐ A description of any assumptions or corrections, such as tests of normality and adjustment for multiple comparisons
☐	☒ A full description of the statistical parameters including central tendency (e.g. means) or other basic estimates (e.g. regression coefficient) AND variation (e.g. standard deviation) or associated estimates of uncertainty (e.g. confidence intervals)
☐	☒ For null hypothesis testing, the test statistic (e.g. *F*, *t*, *r*) with confidence intervals, effect sizes, degrees of freedom and *P* value noted *Give P values as exact values whenever suitable.*
☒	☐ For Bayesian analysis, information on the choice of priors and Markov chain Monte Carlo settings
☒	☐ For hierarchical and complex designs, identification of the appropriate level for tests and full reporting of outcomes
☒	☐ Estimates of effect sizes (e.g. Cohen's *d*, Pearson's *r*), indicating how they were calculated

Our web collection on statistics for biologists contains articles on many of the points above.

Software and code

Policy information about availability of computer code

Data collection	Fluorescent data were collected by Leica Application Suite X software (version 5.2.2). NMR data were collected by VNMRJ (rev.3.2A) software. The MS-data were collected by Thermo Fisher Scientific's Xcalibur (version 4.1) software. Single vesicle data were collected by smCamera from TJ Ha's lab. The multi-electrode array assay data were collected by AxIS Navigator software (version 3.6.2) Axion Biosystems.
Data analysis	Florescent data were analyzed by Leica Application Suite X software (version 5.2.2) and ImageJ (version 1.54i). NMR data were analyzed by SPARKY (version 3.115) and NMRpipe (build 2018). The cross-linked peptide pairs were analyzed and identified by pLink (version 1.9). Single vesicle data were collected by smCamera from TJ Ha's lab. The multi-electrode array assay data were analyzed by Axion BioSystems' AxIS Navigator software and Neural Metric Tool (version 4.1.1).

For manuscripts utilizing custom algorithms or software that are central to the research but not yet described in published literature, software must be made available to editors and reviewers. We strongly encourage code deposition in a community repository (e.g. GitHub). See the Nature Portfolio guidelines for submitting code & software for further information.

Data

Policy information about availability of data

All manuscripts must include a data availability statement. This statement should provide the following information, where applicable:

- Accession codes, unique identifiers, or web links for publicly available datasets
- A description of any restrictions on data availability
- For clinical datasets or third party data, please ensure that the statement adheres to our policy

All data are available in the main text or the extended data. Source data are provided with this paper. The XL-MS raw data and pLink searched data have been uploaded to iProX with the accession number IPX0006924001. Any data supporting the findings of this manuscript are available from the corresponding author upon reasonable request

Research involving human participants, their data, or biological material

Policy information about studies with human participants or human data. See also policy information about sex, gender (identity/presentation), and sexual orientation and race, ethnicity and racism.

Reporting on sex and gender	N/A
Reporting on race, ethnicity, or other socially relevant groupings	N/A
Population characteristics	N/A
Recruitment	N/A
Ethics oversight	N/A

Note that full information on the approval of the study protocol must also be provided in the manuscript.

Field-specific reporting

Please select the one below that is the best fit for your research. If you are not sure, read the appropriate sections before making your selection.

☒ Life sciences ☐ Behavioural & social sciences ☐ Ecological, evolutionary & environmental sciences

For a reference copy of the document with all sections, see nature.com/documents/nr-reporting-summary-flat.pdf

Life sciences study design

All studies must disclose on these points even when the disclosure is negative.

Sample size	The number of experiments, sample size and statistic tests are reported in the respective figure legends. All the in vitro phase separation imaging assays (Fig. 1a,c, Fig. 3a,c, and Extended Data Fig. 1e-g,j) were performed in at least three independent experimental sessions. The EM imaging assays (Fig. 4b, h and Extended Data Fig. 6b) were performed in three independent experimental sessions.
Data exclusions	No data were excluded from the analyses.
Replication	All successful data were generated over multiple attempts and in at least three replicates (replicates number are specified in the manuscript)
Randomization	Experiments randomization was not necessary, but in all experiments, control and experimental samples were analyzed in parallel.
Blinding	Data collection and analysis were not performed blind to the conditions of the experiments.

Reporting for specific materials, systems and methods

We require information from authors about some types of materials, experimental systems and methods used in many studies. Here, indicate whether each material, system or method listed is relevant to your study. If you are not sure if a list item applies to your research, read the appropriate section before selecting a response.

Materials & experimental systems

n/a	Involved in the study
☐	☒ Antibodies
☐	☒ Eukaryotic cell lines
☒	☐ Palaeontology and archaeology
☐	☒ Animals and other organisms
☒	☐ Clinical data
☒	☐ Dual use research of concern
☒	☐ Plants

Methods

n/a	Involved in the study
☒	☐ ChIP-seq
☒	☐ Flow cytometry
☒	☐ MRI-based neuroimaging

Antibodies

Antibodies used

syntaxin-1 (1:1,000, Cat. 110011, SYSY), SNAP-25 (1:1,000, Cat. 111011, SYSY; SMI81 (1:1,000, Cat. 76422-670, Sternberger monoclonals), synaptobrevin-2/VAMP2 (1:2,000, Cat. 104211, SYSY), Emd (detected by GFP antibody, 1:1,000, JL-8, Takara Bio Clontech), α-synuclein (1:2,000, Cat. 610786, BD Transduction), α-tubulin (25 ng/mL, Cat. 12G10, DSHB), GFP (1:1,000, Cat. 632381, Takara Bio Clontech), Hsc70 (1:1,000, P903, in house made), DYKDDDK (Flag) (1:1,000, Cat. 2368S, CST), β-Actin (1:1,000, Cat. ab8227, Abcam), synaptophysin (1:10,000, Cat. 101011, SYSY), Rpt4 (1:500, Cat. sc-65753, SCBT), VDAC (1:1,000, Cat. 4661, CST), SEC61B (1:1,000, Cat. 14648S, CST), P-S129-α-Syn (1:1,000, Cat. 51253, Abcam), Tuj1 (1:1,000, Cat. 302302, SYSY).

Validation

All antibodies are commercially validated. Validation statements found on manufacturer's website indicate the following validations: syntaxin-1, SNAP-25, VAMP2, α-syn, α-tubulin, GFP, DYKDDDK (Flag), β-Actin, synaptophysin, Rpt4, VDAC, SEC61B, P-S129-α-Syn, Tuj1. Each lot of an antibody is tested for conformance with characteristics of a standard reagent and representative western blot data is included in data sheets to demonstrate specificity and/or sensitivity to a relevant cell population. Anti-SNAP25's SMI81 is validated in this paper https://pubmed.ncbi.nlm.nih.gov/22187053/. The Hsc70 is in-house made by Sudhof lab, the antibody identifier is P903, and is validated signal at correct molecular weight.

Eukaryotic cell lines

Policy information about cell lines and Sex and Gender in Research

Cell line source(s)

HEK-293T (Cat.# CRL-3216) cell lines were purchased from ATCC, USA.

Authentication

HKE-293T cells have been authenticated by STR method.

Mycoplasma contamination

The cell line is negative for mycoplasma contamination

Commonly misidentified lines
(See ICLAC register)

We didn't use any commonly misidentified cell lines.

Animals and other research organisms

Policy information about studies involving animals; ARRIVE guidelines recommended for reporting animal research, and Sex and Gender in Research

Laboratory animals

C57/BL6 mixed gender mice used in this paper were purchased from Lingchang Company, Shanghai, China and the Jackson Lab, California, USA. Sprague-Dawley (SD) ratswere purchased from Lingchang Company, Shanghai, China. Alpha/beta/gamma synuclein triple knockout mice were kindly donated by Dr. Thomas C. Südhof (Stanford University, Palo Alto, USA). Synuclein triple knockout mice were bred as homozygous knockout mice.

Wild animals

No wild animals were used in the study.

Reporting on sex

Mixed gender mice for SVs preparation and primary neuron cultures.

Field-collected samples

No field collected samples were used in the study.

Ethics oversight

All animal procedures were performed in accordance with the protocols approved by the Animal Care Committee of the Interdisciplinary Research Center on Biology and Chemistry, Chinese Academy of Sciences (rat protocol number 20230110001; mouse protocol number 20230110005), and to NIH guidelines and approved by the Committee on Animal Care at Weill Cornell Medicine (mouse protocol number 2014-0016).

Note that full information on the approval of the study protocol must also be provided in the manuscript.